



Distribution, Source Apportionment, and Health Risk Assessment of Heavy Metals in Groundwater in a Multi-mineral Resource Area, North China

Wanjun Jiang^{1,2} · Hongwei Liu^{1,2} · Yizhi Sheng³ · Zhen Ma^{1,2} · Jing Zhang^{1,2} · Futian Liu^{1,2} · Sheming Chen^{1,2} · Qinghua Meng^{1,2} · Yaonan Bai^{1,2}

Received: 10 July 2021 / Revised: 13 December 2021 / Accepted: 17 December 2021 / Published online: 24 January 2022
© The Author(s), under exclusive licence to Springer Nature B.V. 2021

Abstract

Heavy metal contamination in groundwater is one of the most severe environmental issues in the area undergoing mining activities, but the underlying sources of heavy metals and the resulting health risk are not fully understood. In this study, 100 shallow groundwater samples and six mining wastewater samples were collected in a multi-mineral resource, North China. The results showed that the distribution of mine ore resources and hydrogeochemical processes were related to the enrichment of Cd, As, Cu, and Ni in groundwater in the piedmont sloping plain, the southwest of the study area, and enrichment of Pb, Zn, and Hg in eastern mountainous and river valley. Water–rock interaction was the primary underlying source of As, Pb, Ni, and Cr(VI) with the non-negligible influence of mining activities, while Cd, Zn, and Hg were potentially originated from the anthropogenic activities (mining or agriculture). A combination of self-organizing map (SOM) and health risk assessment demonstrated the carcinogenic risks of Cd, As, and Cr(VI) to children and adults (exceeding the unacceptable risk level, $1 \times 10^{-6} < CR_{total} < 1 \times 10^{-4}$), particularly in the piedmont sloping plain and mountain valleys. The total carcinogenic risks for children were much higher than adults, which followed the orders as Cr(VI) > As > Cd, whereas the total non-carcinogenic hazard index of Cu, Pb, Zn, Ni, and Hg to children and adults was negligible. Therefore, there was a concern for carcinogenic risk that must be addressed in the multi-mineral resource area, with a particular focus on the Cr(VI) and As as the primary health risk management and control indexes in groundwater.

Keywords Groundwater · Mineral resource · Hydrogeological condition · Health risk assessment · Chromium contamination

Introduction

As a reliable source of drinking water, groundwater is a critical water resource for maintaining the natural ecosystem (Jha et al. 2020; Hua et al. 2015; Jiang et al. 2019). However, groundwater quality is increasingly deteriorating due to the intensive anthropogenic activities (Hua et al.

2015; Li et al. 2017; Zhang et al. 2018), particularly in areas undergoing mining activities such as opencast mining, deep mining or auxiliary projects (Degraff 2007; Feng et al. 2014; Zeng et al. 2018). On one hand, mining wastewater rich in elevated metals such as cadmium (Cd), arsenic (As), chromium (Cr), copper (Cu), lead (Pb), zinc (Zn), nickel (Ni), and mercury (Hg) is mainly formed from weathering, dissolution, leaching, and erosion of massive rock wastes and tailings by the atmospheric rainfall and surface water runoff (Akcil and Koldas 2006; Sun et al. 2014; Kefeni et al. 2017; Zhu et al. 2020). The groundwater beneath mining operations is contaminated as a result of the poor-quality mine wastewater infiltration from the vadose zone to the aquifer in the so-called multi-mineral resources area (replete with a variety of mineral resources in aquifer media and undergoing intensive mining activities) (Newman et al. 2017; Singh et al. 2018; Adamu et al.

✉ Yizhi Sheng
shengyz0330@163.com

¹ Tianjin Center, China Geological Survey (CGS),
Tianjin 300170, China

² North China Center for Geoscience Innovation,
Tianjin 300170, China

³ Department of Geology and Environmental Earth Science,
Miami University, Oxford, OH 45056, USA

2015). On the other hand, the geogenic water–rock interaction and biological processes within the aquifer in the mining areas can also deteriorate the groundwater quality (Qu et al. 2018; Sheng et al. 2016, 2017). Most previous research concentrated on hydrochemistry evolution, distribution and migration of heavy metals, and water quality assessment in mining areas with limited types of mine resources (e.g., coal mine and metal mine) (Bempah and Ewusi 2016; Singh et al. 2018; Jiang et al. 2021a; Zhang et al. 2016). However, the underlying sources of heavy metals and resulting health risk issues induced by multiple exposure pathways in the area with multi-mineral resources and the surrounding area have not been fully uncovered.

The heavy metals can enter the human body through the most suitable pathway, drinking or dermal absorption (Singh et al. 2018; Xiao et al. 2019; Sako et al. 2016; Wang et al. 2019a, b). In addition, in areas using groundwater as irrigation water, the crops and soils may accumulate heavy metals (Hashim et al. 2011; Larson et al. 2013; Nath et al. 2018; Sheng et al. 2021), which can also enter into the human body if they are used as food. These consequences pose significant health risks (e.g., carcinogenic and non-carcinogenic) to regions primarily located in the proximity of mining region (Wu and Sun 2016; Zhou et al. 2019), causing either acute or chronic diseases (Khawal and Mor 2019; Song and Li 2015; Zhou et al. 2019). Although some heavy metals are essential as micronutrients for humans (Goldhaber 2003), a variety of human health issues like damaging neurological system, kidney function, ossification process, dysfunction of liver and renal cortex as well as cancer are associated with high intake of potential toxicity (Lee et al. 2007; Singh et al. 2018). For instance, As can lead to chronic arsenic poisoning through prolonged consumption of groundwater as drinking water, including skin lesions, peripheral neuropathy, diabetes, gastritis, colitis, vascular diseases, and cancer (Cheng et al. 2016; Morales et al. 2000; Guo et al. 2014; He et al. 2021; WHO 2011). Cr (VI), classified as a class A carcinogen (Park et al. 2004; WHO 2014), is a known source of carcinogens and toxicity with great harm to human health (Mohan and Pittman 2006; Huang et al. 2021). Exposure to Cr(VI) has been identified as a cause of gastric, liver, lung, oral, kidney and urinary cancers (Linos et al. 2011; Yuan et al. 2011; Tseng et al. 2018). Anemia, kidney disease, gastrointestinal colic, and central nervous system diseases can occur when the toxic element Pb accumulates in the body above tolerable levels (Pareja-Carrera et al. 2014). The excessive Cu posing significant threats to human health will cause metabolism disorders and even lead to liver cirrhosis (Ameh and Sayes 2019). In consequence, it is of great significance to reveal the harm of heavy metal contaminations to the ecosystem and

human health, which have to be urgently concerned in the mining area (Mukherjee et al. 2020; Gao et al. 2019; Tong et al. 2021; Xiao et al. 2019).

Due to varying hydrogeochemical conditions and complicated contamination sources, the distributions and sources of groundwater heavy metals are difficult to predict, significantly challenging their prevention and risk management (He et al. 2019; Li et al. 2016). Therefore, it is necessary to degrade and categorize the data to accurately explain the relationships between the dependent variables and predictors. The linear dimensionality reduction approach (e.g., principle component analysis) was widely utilized to classify samples in groundwater research (Lorite-Herrera et al. 2008; Moore et al. 2009; Cloutier et al. 2008; Gómez et al. 2008)). However, it cannot build clusters (Haselbeck et al. 2019) and can lead to inadequate interpretation when dealing with nonlinear relationships (Astel et al. 2007; Giraudel and Lek 2001; Lee et al. 2019). Alternatively, a self-organizing map (SOM), which belongs to the domain of unsupervised artificial neural network algorithms, can map high dimensional data to low dimensional space, reveal local relationships between variables, and provide a small number of output neurons (Kim et al. 2020), serving as a promising tool for groundwater quality assessments (Choi et al. 2014; Zhu et al. 2020; Lee et al. 2019; Qu et al. 2021).

As such, eight primary heavy metals (As, Hg, Cd, Cr, Pb, Cu, Ni) and other hydrogeochemical variables in 100 shallow groundwater in a multi-mineral resources area (~ 100 mines including coal mines, gold mines, silver mines, copper mines, lead–zinc mines, etc.), northwestern China were analyzed. The correlation analysis and SOM were collectively used to identify the source apportionment and health risk assessment of heavy metals in groundwater in the multi-mineral resource area.

Study Area

Hydrogeological Conditions

The main types of groundwater in the study area are loose rock pore water and bedrock fissure water. According to the aquifer lithology, groundwater occurrence conditions, and hydrodynamic characteristics, the groundwater is divided into five types: loose rock pore water, clastic rock fissure water, carbonate rock fissure karst water, magmatic rock fissure water, and metamorphic rock fissure water. The loose rock pore water is mainly distributed in the surface rivers and local areas along the river banks in the study area or the mountain valley. The lithology of the aquifer is quaternary gravel, gravel sand and sand layer interbedded with gravel sand loam. The groundwater with shallow buried depth and relatively better water

enrichment is mainly recharged by vertical infiltration of meteoric precipitation and surface runoff, and also from the confluence of groundwater in the mountain valley, followed by infiltration of irrigation. Most groundwater is discharged by runoff downstream along rivers and is exposed in the form of springs in some intermountain valleys except for a small amount of evaporation. In addition, artificial exploitation is another major way to discharge shallow groundwater in the study area. The bedrock fissure water is widely distributed, and its lithology is mainly metamorphic basement granite, Jurassic intrusive granite, metamorphic basement diorite, gneiss, marble, etc. However, the degree of water enrichment is weak, and the groundwater dynamics are affected by the season. The groundwater comes from precipitation infiltration with a short runoff channel and is discharged to the aquifer of the intermountain valley. Therefore, the loose rock pore water is the primary exploitation of agricultural irrigation, industrial production, and domestic water in the study area.

Distribution of Mineral Resources

The study area has various mineral resources, including coal, ferrous metals, non-ferrous metals, precious metals, and non-metallic mineral resources. The large scale and rich resources are coal, iron, gold, and silver ore resources, a small part of lead and zinc, phosphorite, and graphite mineral resources, while the other mineral resources are relatively small in scale or the distribution of ore spots.

The coal resources are primarily located in the southwest and east mining areas of the study area, and the ore-bearing strata of the Early Jurassic Xiahuayuan Formation are the coal-bearing rock series with the broadest distribution, the largest scale and the most abundant resources. Iron mines are mainly distributed in the south and northwest area, followed by the central area, where hematite, magnetite, and titanium-magnet minerals of large scale are developed. The non-ferrous mineral resources (mainly lead–zinc ore, with a few copper and molybdenum ore) are mainly distributed in the southeast. The lithology of ore-bearing strata in the region is mainly amphibolic plagioclase granulite, black cloud plagioclase gneiss, volcanic rock, and pyroclastic rock. Precious metal resources (mainly gold ore) mainly distributed in the central mountainous area are the mineral resources with the broadest distribution area and the largest mining scale in this region (around 1500 km²). Additionally, silver ore resources in the study area are less abundant, and most silver deposits (points) are formed by the symbiotic or associated combination of Ag and other beneficial ore-forming elements (e.g., Pb and Zn).

Materials and Methods

Sample Collection and Geochemical Measurement

In this study, 100 groups of shallow groundwater samples, including irrigation wells, domestic wells, and springs from unconsolidated rock pore aquifer, were collected in June 2020 based on the comprehensive consideration of various factors such as topography, water system characteristics, and groundwater utilization status in the study area. The well depth ranged from 10 to 60 m, with the water level depth ranging from 5.28 to 16.78 m. The spring samples used for domestic water by local residents were collected from 16 sets. In addition, to explore the source of groundwater, six groups of mine wastewater samples including mine tailings pond wastewater, mine drainage, and sewage discharged from the dressing plant, were collected. The distribution of collected samples (including groundwater and mine wastewater) and the groundwater flow direction were shown in Fig. 1.

Shallow groundwater samples were taken by a water pump until the stagnant water in the borehole was pumped out by at least 3 times pumping. pH, temperature (t), electrical conductivity (EC), and dissolved SiO₂ in groundwater were measured in-situ using portable field analyzers produced by CLEAN Instruments (Shanghai ZhenMai Instruments Co., Ltd, Shanghai, China) and HANNA instruments (HANNA Instruments Inc, Italy). The samples used for metal ions measurements were filtered with 0.2 μm membrane filters, acidified using 10% HNO₃ to pH < 2, stored in air-free sampling bottles, and stored in 4 °C freezers before analysis. The samples were immediately transported and tested in the Supervision and Testing Center of North China Mineral Resources, Ministry of Natural Resources. The Cd, Cu, Pb, Zn, Ni, Hg, and As were measured by Inductively Coupled Plasma Mass Spectrometry (ICP-MS, Thermo X series II, Thermo Fisher Scientific, USA). Triplicates were used for metal measurements, and the recovery percentage for each analyzed metal was between 95 and 105%. Additionally, the Cr(VI) was tested by the colorimetric methods following the standard methods for the examination of water and wastewater (State Environmental Protection Administration of China 2002). In the process of sample testing, laboratory ultrapure water was used for the blank sample and the experimental dilutions, and the blank value was far below the detection limits of the adopted methods. The detection limits of measured elements were 0.001 mg/L for Cu, Pb, Ni, Zn, Cd, and Hg, and 0.01 mg/L for As and Cr(VI). In addition, the accuracy and precision (repeatability) of samples were checked by analyzing blank, standard, and groundwater samples. Good repeatability was obtained

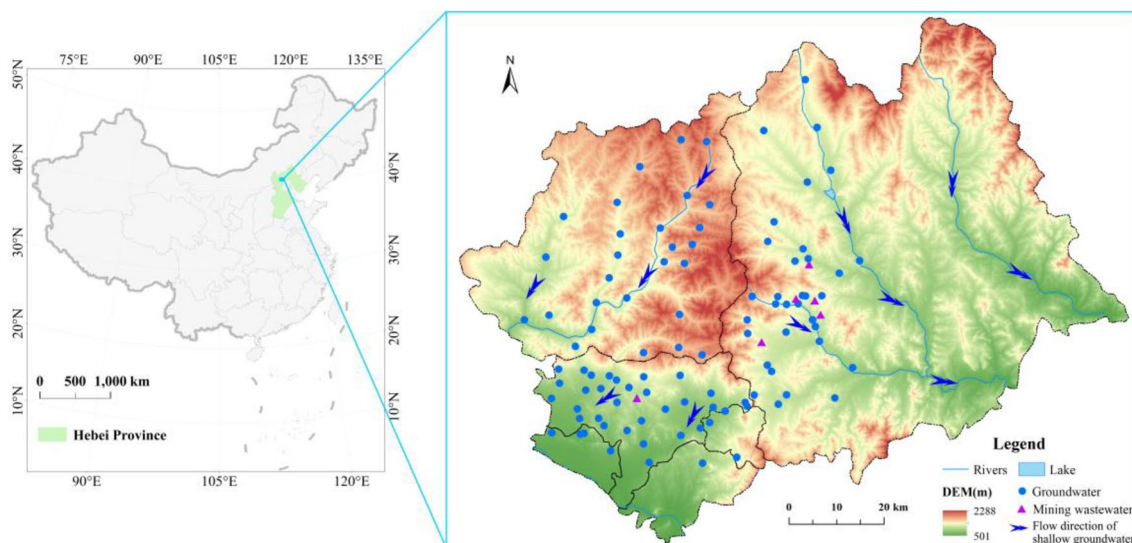


Fig. 1 Sampling location of groundwater and mine waste water and groundwater flow direction in the study area. ‘SG’ represents shallow groundwater

within $\pm 2\%$ standard error. After the initial calibration, a standard was inserted to ensure the data accuracy after every 10 samples.

Major cations (K^+ , Na^+ , Ca^{2+} , Mg^{2+}) were measured with an Inductively Coupled Atomic Emission Spectrometer (ICP-AES, iCAP6300, Thermo Scientific, Waltham, USA). SO_4^{2-} , Cl^- and PO_4^{2-} were measured by Ion Chromatography (DX-120 IC, Thermo Scientific, USA). HCO_3^- was measured by volumetric methods. The F^- was measured by an ion-selective electrode method (Jiang et al. 2021b). NO_3^- , NO_2^- and total Fe were tested by the colorimetric methods following the standard methods (Liu et al. 2020a, b).

Self-Organizing Map (SOM)

As an unsupervised competitive learning neural network method, SOM was designed for the two tasks of unsupervised classification and nonlinear dimensionality reduction in analyzing a large multivariate dataset (Kohonen 1982). SOM can map the high-dimensional input data to low dimensional space while retaining the topology of the input data in high dimensional space. The similar sample points in high dimensional space could be mapped to the neighboring neurons in the two-dimensional output layer (2D); therefore, SOM was widely employed for data dimension reduction, mining and rule summary, such as in hydrology (Chen et al. 2018; Zhu et al. 2020). It constructs its own network structure by simulating the response of human brain neurons to external stimuli and forms a cluster area near each most matched neuron to classify the input vectors with similar features into a cluster.

Heuristic rules such as the empirical Eq. 5 \sqrt{n} suggested by Vesanto et al. (2000) can be used to select the appropriate number of neurons in the neural matrix, where n is the number of samples. Additionally, the Davies-Bouldin Index can be used to determine the optimal number of clusters (Wang et al. 2017a, b; Park et al. 2014). The SOM calculation process was executed using MATLAB software according to the method described by Li et al. (2020). Unified distance matrices (U-matrix) and median distance matrices (D-matrix) are standard tools for displaying SOM clustering structures (Kim et al. 2020). Specifically, the U-matrix denotes the Euclidean distance between the weight vectors of adjacent neurons on the map in the color scale, while the D-matrix represents the median distance between SOM neurons. In the U-matrix, the color represents the weight vector of each neuron, and the weight vector value corresponds to the standardized value of the original data. The same or similar color gradient indicates a positive correlation and the higher the degree of similarity (Lee et al. 2019; Jampani et al. 2018; Dai et al. 2018). In addition, neurons with low distance (i.e., high similarity) can be regarded as a cluster, while neurons with high distance (i.e., low similarity) can be regarded as the cluster boundary (Kim et al. 2020).

Health Risk Assessment Model

The health risk assessment takes the risk degree as the evaluation index and uses the combination of environmental quality and human health to quantitatively evaluate the potential health risk of hazardous substances to the human body (Giri and Singh 2015; Liu et al. 2010). The health risk assessment

model for the water environment proposed by the United States Environmental Protection Agency (USEPA 2017) was employed. Health risks of heavy metals to adults and children in shallow groundwater were assessed according to relevant technical requirements in China's Technical Guidelines for Risk Assessment of Contaminated Sites (HJ 25.3-2014) (CHNMEP 2014). It is generally believed that small amounts of carcinogenic chemicals, also known as genotoxins in water, can pose a severe health risk to human bodies. Also, the potential hazard of non-carcinogenic substances known as somatotoxins to human health cannot be neglected. This study determined the different evaluation indexes combined with the information provided by the International Agency for Research on Cancer (IARC 2013) and the World Health Organization (WHO 2011) on the hazardous effects of different toxic chemicals on human health. Therefore, the model we used included the health risk assessment of chemical carcinogens, i.e., Cd, As, Cr(VI), and non-carcinogenic substances, i.e., Cu, Pb, Zn, Ni, and Hg.

Exposure Assessment

Dose–Response Assessment

The main routes of human exposure to heavy metals or metal-like substances in the environment generally include oral ingestion, dermal contact, and inhalation (Lee et al. 2013). Among these pathways, oral ingestion (e.g., water and food) and dermal contact are two of the most common ones (Giri et al. 2014; Kim et al. 2004; Li et al. 2010; Miguel et al. 2007; Ravindra et al. 2019; Zhou et al. 2021). Therefore, since groundwater in the study area is used as domestic and irrigation water, the present study assessed the potential health risks for adults and children in shallow groundwater with different physiological conditions through

oral ingestion and dermal contact routes. Different methods calculated the exposure dose for different routes according to the health risk assessment model recommended by the USEPA.

The calculation model for the exposure dose of the oral ingestion route was shown as Eq. 1.

$$I_{\text{oral}} = \frac{C_{\text{water}} \times \text{IR} \times \text{EF} \times \text{ED}}{\text{BW} \times \text{AT}} \quad (1)$$

The calculation model for the exposure dose of the dermal contact route was shown as Eq. 2.

$$I_{\text{dermal}} = \frac{C_{\text{water}} \times \text{SA} \times K_p \times \text{ET} \times \text{EV} \times \text{EF} \times \text{ED} \times \text{CF}}{\text{BW} \times \text{AT}} \quad (2)$$

where I_{oral} and I_{dermal} represent the average daily exposure dose of drinking water and dermal contact route [mg/(kg d)], respectively. C_{water} is the measured concentration of heavy metals in water (mg/L). IR represents the daily ingestion rate of water (L/d). EF is the exposure frequency, the time of exposure in one year (d/y). ED represents the duration of exposure, indicating the number of years that the substance is ingested in the body during its lifetime (y). BW is the average weight of residents (kg). AT is the average exposure time, i.e., the life expectancy of residents (d). SA is the surface area of dermal contact at a dose of heavy metals. K_p is the skin permeability coefficient of the different indexes (cm/h). EV is the daily exposure frequency (1 in this study). ET is the contact duration (h/d). CF is a conversion factor (0.001 L/cm³). The exact values of each parameter were shown in Table 1.

Table 1 Parameters of health risk assessment model

Parameters	Symbol	Unit	Children	Adult	References
Concentration water intake	C_{water}	mg/L	Measured value	Measured value	Measured value Li et al. (2016), He et al. (2021), Wu and Sun, (2016), Wu et al. (2019)
	IR	L/d	0.7	1.5	
Exposure frequency	EF	d/y	350	350	Zeng et al. (2015), Tong et al. (2021), CHNMEP (2014)
Exposure duration	ED	y	6	24	CHNMEP (2014)
Body weight	BW	kg	15	70	Li et al. (2021), Tong et al. (2021), USEPA, (2013)
Exposure time	AT	d	365 × ED (Non-carcinogenic)	365 × ED (Non-carcinogenic)	USEPA (2004, 2011), Li et al. (2016)
			365 × 70 (Carcinogenic)	365 × 70 (Carcinogenic)	
Superficial area	SA	cm ²	6600	18,000	USEPA (2004), Wang et al. (2017a, b), Xiao et al. (2019), Zeng et al. (2015)
Contact duration	ET	h/d	1	0.58	Wang et al. (2017a, b), Xiao et al. (2019)
Conversion factor	CF	L/cm ³	0.001	0.001	Li et al. (2016), Wu and Sun (2016)

Table 2 Reference values of K_p , SF and RfD for health risk assessment model

Classes	Element	K_p cm/h	SF [mg/(kg d)] ⁻¹		RfD [mg/(kg d)]	
			Oral ingestion	Dermal contact	Oral ingestion	Dermal contact
Carcinogenic substances	As	0.001	1.5	3.66	–	–
	Cd	0.001	6.1	0.38	–	–
	Cr(VI)	0.003	0.5	20	–	–
Non-carcinogenic substances	Cu	0.001	–	–	0.04	0.012
	Hg	0.001	–	–	0.0003	0.000021
	Ni	0.004	–	–	0.02	0.0054
	Pb	0.001	–	–	0.0035	0.000525
	Zn	0.0006	–	–	0.3	0.06

Date from USEPA (2004, 2011), Baltasa et al. (2020), Jiang et al. (2017), Pan et al. (2018), Chen et al. (2015), Zeng et al. (2015), and CHNMEP (2014)

Risk Characterization

According to the health risk assessment model, the calculation methods of the potential risks for chemical carcinogenic and non-carcinogenic substances to human health under the same exposure pathway are distinct, where carcinogens are characterized by carcinogenic risk (CR), and non-carcinogenic risks are characterized by non-carcinogenic hazard quotient (HQ) and hazard index (HI).

The carcinogenic risk caused by carcinogens through oral ingestion and dermal contact route was calculated as shown in Eqs. 3–5.

$$CR_i = I_{\text{oral}} \times SF_o + I_{\text{dermal}} \times SF_d \quad (3)$$

$$CR_i = 1 - \exp(-I_{\text{oral}} \times SF_o) + 1 - \exp(-I_{\text{dermal}} \times SF_d) \quad (4)$$

$$CR_{\text{total}} = \sum_{i=1}^n CR_i \quad (5)$$

For carcinogenic risk assessment, the value of carcinogenic risk was calculated by Eq. 4 when $I_{\text{oral}} \times SF_o$ or $I_{\text{dermal}} \times SF_d > 0.01$ (Li et al. 2014; USEPA 2017; Yang et al. 2015). The total carcinogenic risk CR_{total} of various carcinogens was calculated by Eq. 5. Where CR_i is the health risk value of carcinogenic index i , I_{oral} and I_{dermal} are calculated by the Eqs. 1 and 2 and SF is the carcinogenic slope factor for chemicals [mg/(kg d)]⁻¹.

The health risk caused by non-carcinogenic substances through oral ingestion and dermal contact route was calculated as shown in Eqs. 6 and 7.

$$HQ_j = \frac{I_{\text{oral}}}{\text{RfDo}} + \frac{I_{\text{dermal}}}{\text{RfDd}} \quad (6)$$

$$HI = \sum_{j=1}^n HQ_j \quad (7)$$

where HQ_j is the hazard quotient of non-carcinogenic index i , HI is the comprehensive/total risk value of various non-carcinogenic indicators and RfD is the reference dose for chemicals [mg/(kg d)].

In this study, the acceptable level of carcinogenic risk was 1×10^{-6} . When the CR_{total} is less than 1×10^{-6} , the carcinogenic risk is considered to be nonexistent or low. When $1 \times 10^{-6} < CR_{\text{total}} < 1 \times 10^{-4}$, it indicates a possible carcinogenic risk. When $CR_{\text{total}} > 1 \times 10^{-4}$, the level of potential carcinogenic risk is considered unacceptable (Duan and Zhao 2014; Fryer et al. 2006; Guney et al. 2010; Ravindra et al. 2019; Ravindra and Mor 2019). In addition, if HQ and HI are less than 1, the non-carcinogenic health risk caused by the chemical substance is considered to be an acceptable level. Otherwise, it is unacceptable, and the level of non-carcinogenic health risks tend to increase with the increase of HI (Chen et al. 2016; Li et al. 2016; Ravindra et al. 2019; Ravindra and Mor 2019; Wu and Sun 2016; Yang et al. 2015).

Model Parameters

The carcinogenic slope factor SF and the reference dose RfD of heavy metals in the health risk assessment model were obtained based on the recommended values of the USEPA. However, the application conditions of the model may be different from the actual situation. Thus, the exposure parameters were appropriately adjusted by referring to the local Technical Guidelines HJ 25.3-2014 (CHNMEP 2014) and published literature to ensure that the human health risk assessment results were relatively consistent with the actual situation of the study area. The

Table 3 The statistics of heavy metals and other hydrochemical parameters in groundwater

Parameter	Unit	Min	Mean	Max	Q ₁	Median	Q ₃
Cd	µg/L	0	0.028	0.75	0.002	0.007	0.015
As	µg/L	0	0.641	5.38	0.34	0.5	0.765
Cr(VI)	µg/L	0	4.178	54.7	0	2.285	5.675
Cu	µg/L	0	0.485	12.1	0.099	0.16	0.28
Pb	µg/L	0	0.093	1.26	0.007	0.03	0.086
Zn	µg/L	0	0.217	6.58	0.021	0.044	0.155
Ni	µg/L	0.86	2.755	24.9	1.88	2.495	3.005
Hg	µg/L	0	0.023	0.27	0.015	0.018	0.023
t	°C	6.9	11.8	18.8	8.95	11.15	14.7
pH	–	7.12	7.67	8.41	7.56	7.69	7.8
EC	mS/cm	0.19	0.51	0.86	0.42	0.5	0.62
K ⁺	mg/L	0.37	2.68	8.61	1.76	2.62	3.46
Na ⁺	mg/L	5.44	15	51.76	7.53	11.72	17.58
Ca ²⁺	mg/L	30.4	65.5	90.3	58.6	65.42	75.38
Mg ²⁺	mg/L	2.05	17.2	39.43	11.09	15.61	23.95
Cl ⁻	mg/L	2.96	16.9	53.2	8.87	12.6	20.3
SO ₄ ²⁻	mg/L	6.66	50.7	148.9	25.86	37.86	62.63
HCO ₃ ⁻	mg/L	73.4	204	287	186	209.5	249
NO ₃ ⁻	mg/L	0.03	22.4	80	7.11	22.05	30.7
NO ₂ ⁻	mg/L	0	0.03	0.29	0.01	0.01	0.02
F ⁻	mg/L	0.27	0.76	1.64	0.55	0.7	1.01
SiO ₂	mg/L	0.84	2.99	20.6	1.32	1.55	1.84
PO ₄ ³⁻	mg/L	0.02	0.23	4.28	0.09	0.11	0.14

Q₁ and Q₃ represent the Upper and Lower quartile, respectively

exact reference values of each parameter in the model were shown in Tables 1 and 2.

Results and Discussion

Heavy Metal Distribution in Groundwater

The single component assessment of groundwater, based on the national standard of ‘the People’s Republic of China: Quality standard for groundwater’ (GB/T14848-2017), was employed to determine whether the groundwater was acceptable for drinking or industrial and agricultural uses. To be noted, this assessment only considered the perspective of the selected heavy metals. Its principle is that the groundwater should be regarded as unsuitable for drinking water resources or industrial and agricultural uses if any index exceeds the standard of Grade III, equivalent to the drinking water standard (GB 5749-2006) (CHNMH 2006). The Cr(VI) (54.7 µg/L) and Ni (24.9 µg/L) in two samples exceeded the standard of Grade III, while the other groundwater samples met the standard (Fig. S1, Table 3). Therefore, from the perspective of the selected heavy metals, the shallow groundwater quality was generally suitable for irrigation and drinking.

However, the presence of As, Hg, Cr(VI), Cd and Pb etc., may still cause significant adverse effects on human health due to their high toxicity, even at low concentrations (Jia et al. 2018; Muhammad et al. 2011; Podgorski et al. 2017; Riederer et al. 2013; Singh et al. 2018). Although trace elements such as Cu, Zn, and Ni are essential for metabolic processes in plants, animals, and microorganisms, long-term exposure of these metals to human result in accumulated health risks in areas where groundwater is the main source of drinking water (Bodrud-Doza et al. 2019; Dieter et al. 2005; Fang et al. 2021).

The spatial distribution of the investigated heavy metal contents in the groundwater exhibited regional differences (Fig. 2). Samples with high Cd concentrations were mainly distributed in the river valley in the northwest and the piedmont sloping plain in the southwest of the study area. In contrast, samples with relatively high Cr concentrations were distributed in the river valley in the northwest, and a few samples were located in the east of the mountain valley. The distribution of Pb and Zn in groundwater was similar, mainly distributed in the northwest and east river valley and a small amount in the piedmont sloping plain in the southwest. Cu, As, Ni, and Hg distributions were also similar, mainly distributed in the northwest and east river valley, and the other high concentrations were sporadically distributed

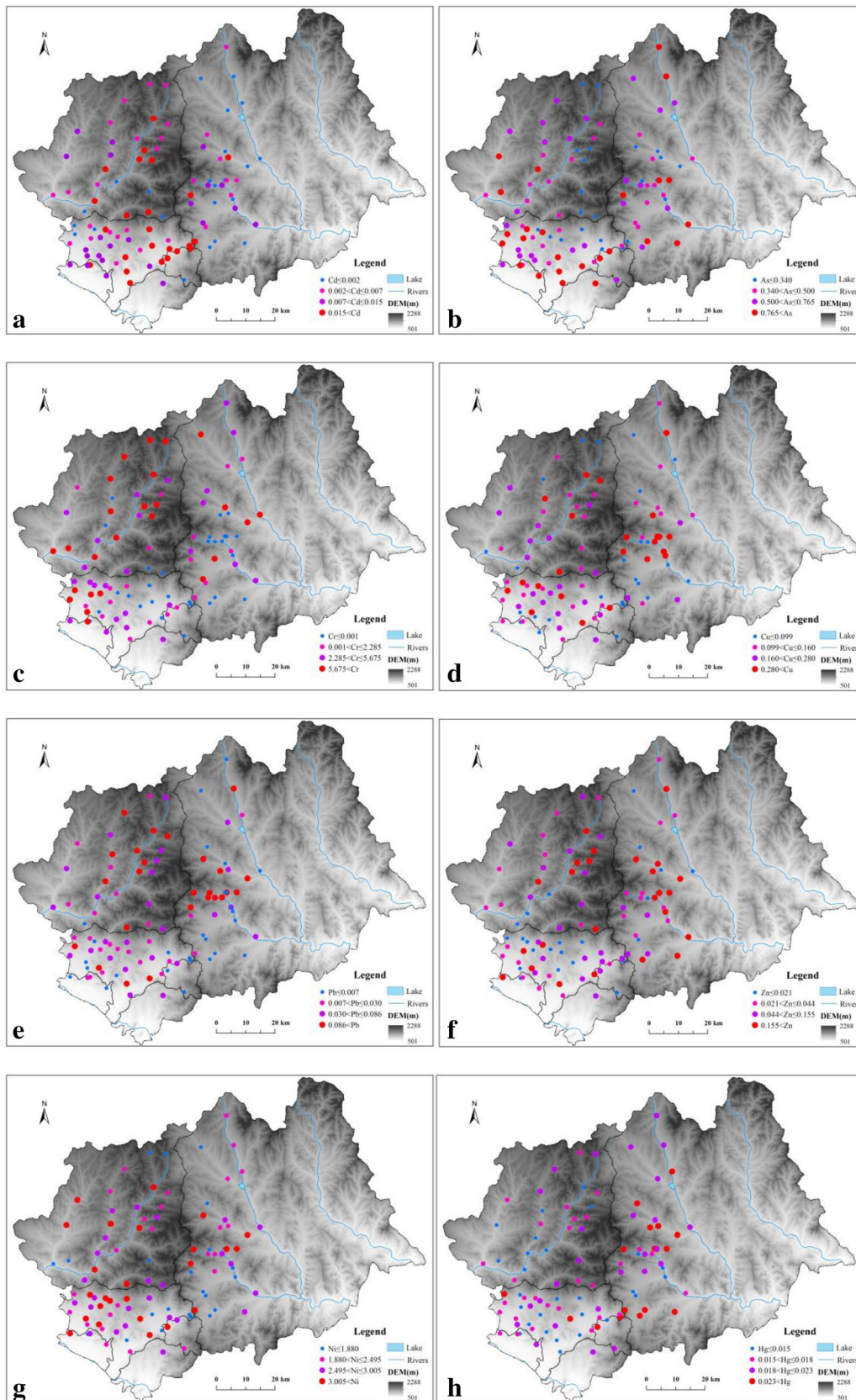


Fig. 2 Distribution characteristics of eight heavy metals in groundwater

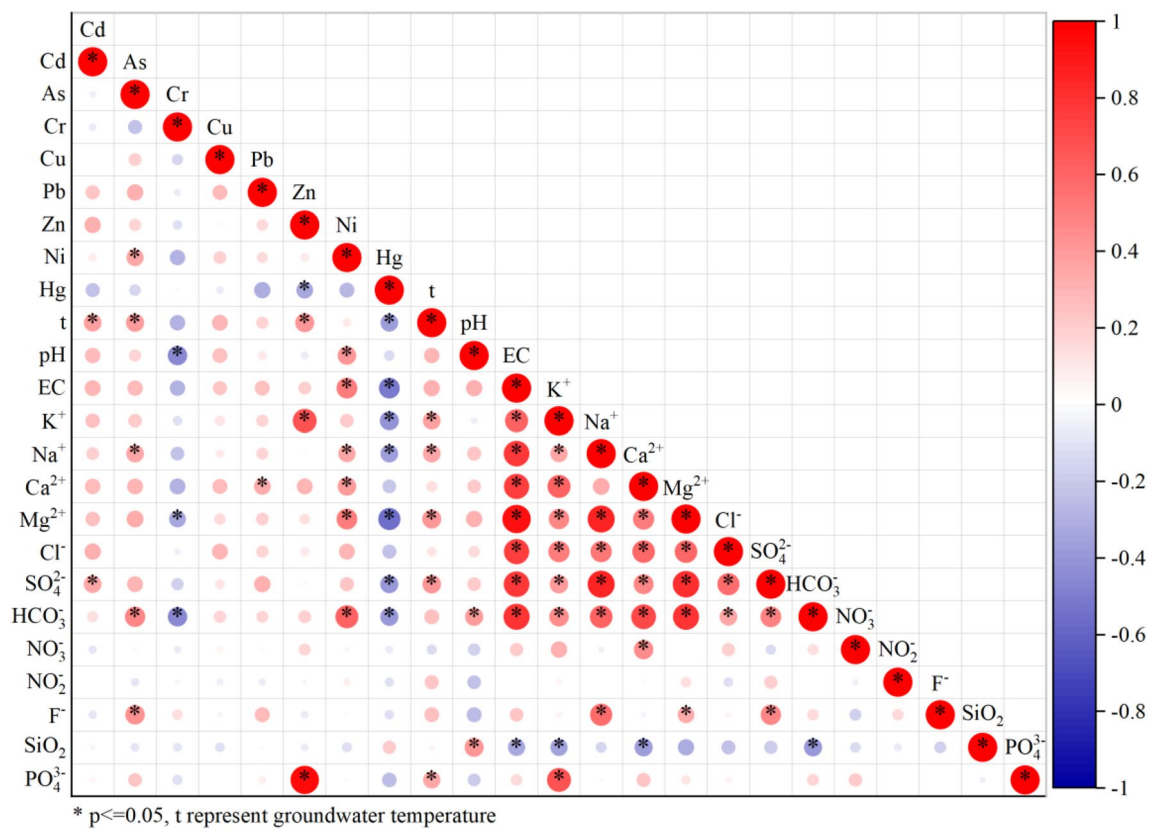


Fig. 3 Pearson correlation analysis between heavy metals and other parameters in groundwater. The colors represent the correlation coefficient, increasing from blue (negative) to red (positive). Bubble size

represents the correlation coefficient (r), increasing from small size to large size. The bubble with an asterisk in it represents the significant correlation ($p \leq 0.05$)

in the northwest mountainous region. Additionally, the Cr, Pb, and Zn contents of groundwater samples in the river valley in the northwest of the study area were relatively high. To sum up, groundwater in the piedmont sloping plain in the southwest of the study area harbored the high concentrations of Cd, As, Cu, and Ni, and groundwater in the eastern mountainous and river valley harbored the high Cu, Pb, Zn, Ni, and Hg concentrations.

To further study the potential source of heavy metals in groundwater, the contents of heavy metals in some mine wastewater samples were measured and shown in Table S1. The contents of Pb and As in the disposal sewerage collected from the gold concentrator were relatively high, with 53.4 $\mu\text{g/L}$ and 11.8 $\mu\text{g/L}$, respectively, which were 5.34 and 1.18 times higher than the standard of Grade III (local groundwater standard), indicating a potential contamination source. Meanwhile, Pb, Hg, and Ni contents in samples collected from iron mine drainage were high with 12.5 $\mu\text{g/L}$, 3.76 $\mu\text{g/L}$, and 53.4 $\mu\text{g/L}$, which were 1.25, 3.76, and 2.67 times higher than the local groundwater standard. The mining residues and wastewater in the mine tailings pond and concentrators could pose a threat to the surrounding pristine

groundwater, likely resulting in potential health risks to residents in the mining area.

The distributions of heavy metals can be related to hydrogeochemical conditions in the study area. Mountain and river valleys are relatively concentrated distribution areas of mineral resources, the recharge area of regional groundwater. The recharge conditions of unconfined groundwater are good due to large lithologic particles in the aquifer and short runoff paths in these large topographic slope regions (Fig. 2). Most meteoric waters recharge the shallow groundwater by dispersing vertical infiltration after leaching and dissolving rocks and minerals. Therefore, heavy metals were relatively easy to enter shallow groundwater during the infiltration recharge process. However, heavy metals were not easily enriched in the groundwater due to the fast cycle alternating frequency in this area. In the plains, shallow groundwater is under worse runoff conditions with slow circulation alternates because of gentle terrain and finer lithologic particles, whereas there are few potential pollution sources of groundwater due to the mineral resources in this area. The quaternary loose sediments with different thicknesses are widely distributed overlying the aquifer, constituting a thick unsaturated zone. The lithology is mostly clay and silty clay

with fine particle size and low porosity. Thus, the content of heavy metals may be trapped in the unsaturated zone (Sheng et al. 2021), leading to relatively low heavy metal concentrations in the groundwater (Table 3).

Correlation Analysis Between Heavy Metals and Other Hydrogeochemical Parameters

The As and Cr are widely distributed in the Earth's crust (Facchinelli et al. 2001; Šajin et al. 2011), and infiltrated into the groundwater via the leaching process. As shown in Fig. 3, As was significantly correlated with Ni at the level of 0.05, indicating that the sources of As and Ni in groundwater were similar. However, the correlation between As, Ni, and other heavy metals was low, indicating that the sources for other heavy metals were different from As and Ni. The Pearson correlations analysis showed that As was positively correlated with temperature, Na^+ , HCO_3^- and F^- , and Ni was positively correlated with pH, EC, Na^+ , Ca^{2+} , Mg^{2+} , and HCO_3^- (Fig. 3), which were the main ionic component of natural groundwater. The F^- is mainly affected by the weathering and dissolution of fluoride-rich minerals in natural groundwater, thus it is easy to enrich in the groundwater environment with high Na^+ and HCO_3^- (Feng et al. 2020; Li et al. 2019; Su et al. 2019; Wang et al. 2021; Wu et al. 2018). Therefore, the results indicated that the sources of As and Ni in groundwater were similar to Na^+ , HCO_3^- and F^- , which was mainly weathering and dissolution of surrounding rock minerals in aquifers, i.e., water–rock interactions controlled the source and distribution of the ions. However, because high concentrations of As and Ni have been found in the mining wastewater (Table S1), the As and Ni in groundwater may also be affected by mining activities. In addition to the natural sources, anthropogenic sources of Cr can also be important, including metallurgy, refractory, and chemical manufacturing (Rakhunde et al. 2012). Cr(VI) was negatively correlated with pH, Mg^{2+} and HCO_3^- in groundwater (Fig. 3), indicating that pH, Mg^{2+} , and HCO_3^- restricted the enrichment of Cr(VI) in groundwater to a certain extent. Previous studies have demonstrated that pH is a critical driving force governing the distribution of heavy metals. For instance, under different pH conditions, the adsorption and desorption of As (Huang and Matzner 2006; He et al. 2021; Khaska et al. 2018; Lidman et al. 2011; Sun et al. 2020; Wang et al. 2018) or Cr (Dermatas et al. 2015; Muhammad et al. 2011; Robles-Camacho and Armienta 2000) to minerals are important in their occurrences. The bioreduction of Cr(VI) with inorganic electron donors (e.g., elemental sulfur) was also reported to increase the groundwater pH values (Zhang et al. 2021). Likely because pH values in groundwater are circum-neutral or slightly alkaline with a low variation in the present study (7.12–8.41) (Table 3), pH did not display strong correlations with other heavy metals (Fig. 3).

To be noted, although the enrichment of Pb in groundwater is mostly human-induced, such as the release of pesticide, leadstorage batteries, gasoline additives, or fire coal (Emenike et al. 2020; Shil and Singh 2019; Siddiqui et al. 2020; Singh and Kumar 2017), The significant positive correlation between Pb and Ca^{2+} (Fig. 3) indicated that Pb entered the groundwater probably due to the reaction between galena and carbonated water (Liao et al. 2018). As lead and zinc deposits were rich in the study area, the source of Pb in groundwater could be the weathering and dissolution of surrounding rock minerals. However, the Pb was also enriched in the area where mine wastewater samples with high Pb concentrations were collected, thus the cause of mining activities cannot be ruled out (Table S1). To sum up, the contents of As, Pb, Ni, and Cr(VI) in groundwater were mainly controlled by the weathering and dissolution of surrounding rock minerals (Khodapanah et al. 2009; Ravindra and Garg 2007; Wang et al. 2016), and might be affected by groundwater environment or human activities in the mining areas.

Cd in groundwater generally results from greenockite and/or industrial wastes and pesticides or fertilizers (Lv et al. 2015; Zhao et al. 2004). Although Cd was positively correlated with SO_4^{2-} (Fig. 3), sulfur-bearing greenockite deposits were not distributed in the study area. Moreover, the correlation between Cd and other heavy metals and groundwater chemical components was non-significant (Fig. 3). Thus, the source of Cd in the groundwater might not be the leaching of natural surrounding rock minerals but should be more likely the human-induced sources such as the use of agricultural fertilizer, especially phosphate fertilizer (Zhao et al. 2004). Moreover, Zn was positively correlated with K^+ , and PO_4^{3-} (Fig. 3), but not with the main chemical components of groundwater (cations and ions). As shown in Table S1, the contents of Cd and Zn in the mining wastewater were low, underlying that the source of Cd and Zn could result from other sources such as agricultural activities, i.e., the use of pesticides, fertilizers, or animal waste (Lv et al. 2015; Zhao et al. 2004). Hg was negatively correlated with Zn, temperature, EC, K^+ , Na^+ , Mg^{2+} , SO_4^{2-} , and HCO_3^- (Fig. 3), indicating that the sources of Zn and Hg and the factors affecting their migration and transformation in groundwater were inconsistent. Because Hg was high in the mine wastewater (Table S1), the influence of mining activities on the Hg content in groundwater was a potential source.

Clustering of Sample Sites by SOM

Self-organizing map (SOM) was employed to classify the groundwater samples based on the concentrations of heavy metals. 50 (5×10) neurons and 4 clusters were selected according to Heuristic rules and Davies–Bouldin index, and the results were shown in Fig. 4a. The samples in each

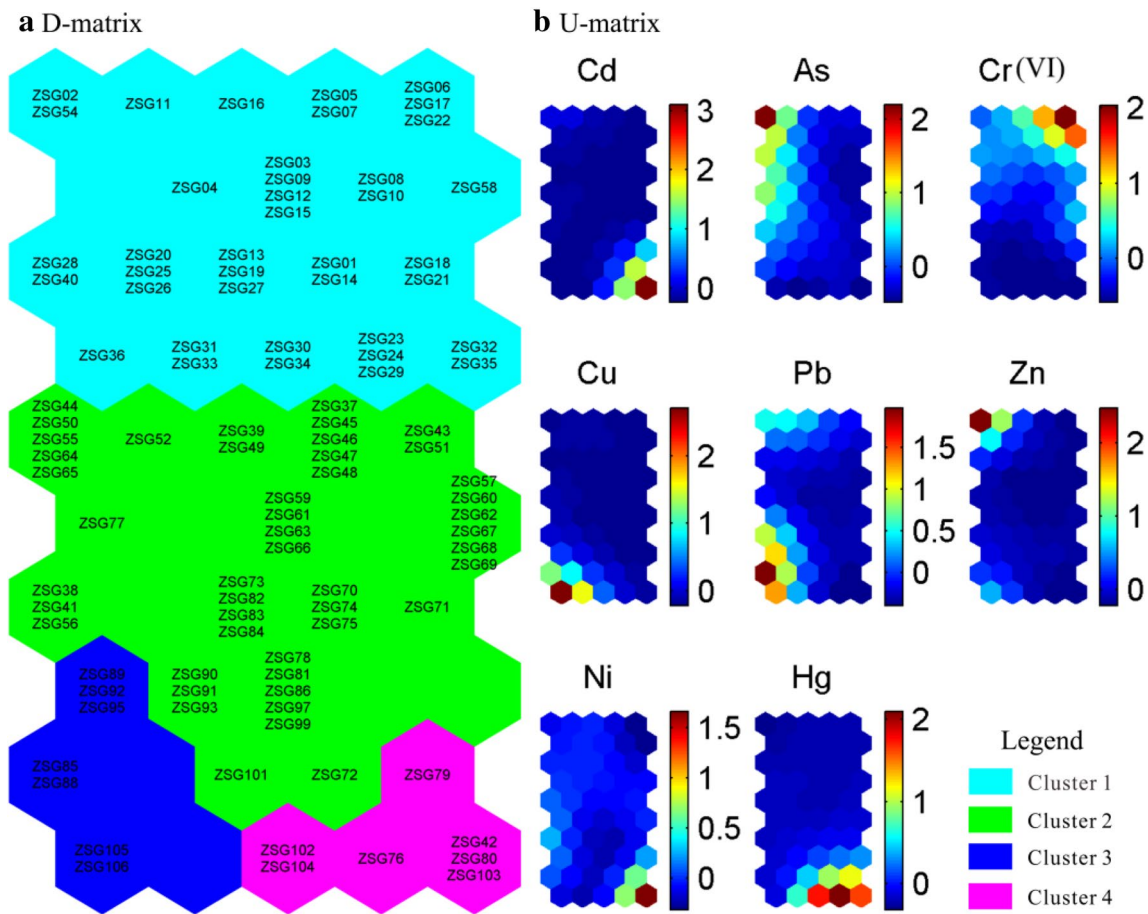


Fig. 4 **a** The SOM matrix map of groundwater samples: the clustering pattern in the SOM, different colors represent different clusters and the number in a hexagon denotes the sample number. **b** result

of the SOM visualization of corresponding variables. The blue and red colors correspond to low and high values, respectively, which can detect the correlation between variables

cluster likely had similar distribution characteristics and sources of heavy metals in groundwater. Each U-matrix map represented an index value obtained after dimension reduction, as marked by shades of blue to red (Lee et al. 2019; Zhu et al. 2020). The neurons with high values or low values were shown in red or blue, respectively. After that, informative and qualitative relations among the parameters were intuitively shown by comparing SOM graphs according to the color gradient. The color change gradients of Cd, Ni and Hg were similar, indicating that these 3 indexes have positive correlations (Fig. 4b). Similarly, As and Zn or Cu and Pb also had similar color change gradients, suggesting the factors affecting their content and distribution in groundwater were similar to some extent. The SOM results demonstrated that the correlation of heavy metal indexes belonging to the same cluster in groundwater samples hinged on the similarity of their spatial distribution.

Cluster 1, defined by the heavy metal indexes As, Cr(VI), and Zn was located at the top of the D-matrix map in the SOM results (Fig. 4a). Those groundwater samples were

mainly located in mountainous valleys in the west and southwest of the study area (Fig. S2), possibly affected by the weathering and dissolution of surrounding rock minerals.

Cluster 2 was located on the lower side of Cluster 1 (Fig. 4a), in the middle and lower part of the D-matrix, and was dominated by As, Cr(VI), and Pb with the relatively low weight vector values of each component index. It indicated that the groundwater samples had relatively low metal contamination. As shown in Fig. S2, these samples were from the mountainous valleys in the eastern mountain valleys and the upper part of the southwestern piedmont sloping plain in the study area.

Cluster 3, mainly comprised of Cu and Pb, was located in the lower-left part of the D-matrix. These samples were located near the mountainous region in the middle of the study area and close to the mining wastewater samples (Fig. S2), which represented the groundwater was affected by the weathering and dissolution of copper-bearing and lead-bearing minerals in the aboveground mine tailings.

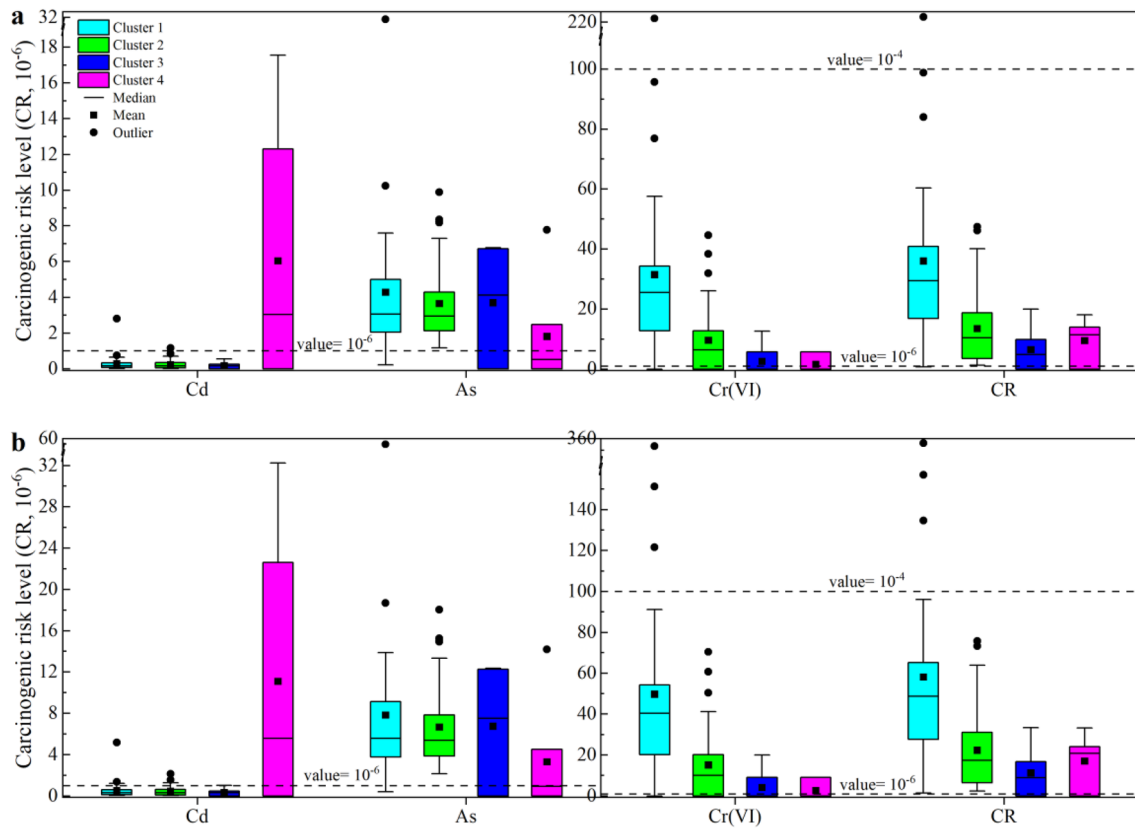


Fig. 5 Box diagram of carcinogenic risk value of different heavy metals in groundwater: **a** and **b** represent the carcinogenic risk for children and adults of each cluster respectively

Cluster 4 was located at the lower right corner of the D-matrix and characterized by Cd, Ni, and Hg. The samples in the Cluster 4 were scattered in the vicinity of the central mountain and the upper part of the alluvial plain in the southern mountain of the study area, and were also near the mine waste water.

Health Risk Assessment

The comprehensive assessment of groundwater quality is an essential prerequisite to ensure the ecological security of the regional water environment and residents' health in the water-shortage region (Mazhar et al. 2019). Based on the SOM results, the health risk assessment was conducted independently for each cluster.

Carcinogenic and Non-carcinogenic Risk Assessments

The potential carcinogenic hazards to both children or adults caused by Cd, As, and Cr(VI) in all clusters had high levels of risk ($CR > 10^{-6}$) (Fig. 5). Cr(VI) had the highest potential carcinogenic health risk level among the four clusters for both children and adults, especially in Cluster 1 (Fig. 5).

Similarly, previous studies have found that Cr(VI) in some shallow groundwater environments was the main source of heavy metal health risks for residents (He, et al. 2019; Singh et al. 2018; Zhang and Wang 2021; Zhou et al. 2021). However, other groundwater studies in some mining area did not suggest the most significant role of Cr in creating groundwater health risk (Bempah and Ewusi 2016; Giri and Singh 2016), and alternatively, the As was suggested as the highest risk index. As had the second highest carcinogenic risk level in the present study, while the level of Cd was the lowest (risk level $< 10^{-6}$ in most samples) except for samples in Cluster 4. These results were consistent with a coal mine (Jiang et al. 2021a), but were inconsistent with other mining areas where one of these parameters had the carcinogenic risk (Giri and Singh 2016; Zhang et al. 2016). The health risks of heavy metals in the groundwater samples of each cluster were shown in Table 4. The overall total carcinogenic risk level (CR) of each cluster followed the order: Cluster 1 > Cluster 2 > Cluster 4 > Cluster 3, and overall CR of heavy metals followed the order: Cr(VI) > As > Cd for both children and adults (Fig. 5).

The non-carcinogenic health risk assessment of heavy metals in groundwater was shown in Fig. 6. The highest

Table 4 Health risks of heavy metals in the groundwater samples from each cluster

	Children											
	Cluster 1			Cluster 2			Cluster 3			Cluster 4		
	Mean	Q1	Median	Q3	Mean	Q1	Median	Q3	Mean	Q1	Median	Q3
Cancer risk(10⁻⁶)												
Cd	0.28	0.07	0.16	0.33	0.24	0.05	0.16	0.35	0.17	0.00	0.16	0.26
As	4.28	2.06	3.06	5.00	3.66	2.12	2.94	4.30	3.70	0.00	4.12	6.71
Cr	31.46	12.75	25.55	34.34	9.60	0.00	6.38	12.75	2.63	0.00	0.00	5.72
CR	36.03	16.88	29.43	40.86	13.49	3.54	10.37	18.77	6.50	0.00	4.87	9.91
Non-cancer risk(10⁻³)												
Cu	0.21	0.12	0.18	0.25	0.26	0.11	0.17	0.31	4.43	0.35	0.77	13.50
Pb	1.03	0.15	0.42	1.25	0.87	0.10	0.37	0.99	6.39	0.00	4.08	15.49
Zn	0.05	0.00	0.01	0.03	0.02	0.00	0.01	0.03	0.08	0.00	0.02	0.09
Ni	6.30	5.00	6.37	7.68	6.56	4.92	6.35	7.34	7.72	4.21	7.90	9.08
Hg	2.82	2.37	2.88	3.05	3.29	2.54	3.39	3.89	2.68	0.00	3.05	4.57
HI	10.41	8.94	10.74	11.84	11.00	9.10	10.23	12.17	21.29	17.99	18.30	27.22
Adults												
	Cluster 1			Cluster 2			Cluster 3			Cluster 4		
	Mean	Q1	Median	Q3	Mean	Q1	Median	Q3	Mean	Q1	Median	Q3
	Mean	Q1	Median	Q3	Mean	Q1	Median	Q3	Mean	Q1	Median	Q3
Cancer risk(10⁻⁶)												
Cd	0.52	0.13	0.30	0.6	0.44	0.09	0.30	0.64	0.32	0	0.30	0.47
As	7.82	3.76	5.59	9.13	6.67	3.87	5.37	7.85	6.76	0	7.52	12.25
Cr	49.75	20.17	40.40	54.3	15.18	0	10.08	20.17	4.16	0	0	9.05
CR	58.10	27.71	48.79	65.24	22.29	6.47	17.37	31.17	11.23	0	8.90	16.7
Non-cancer risk (10⁻³)												
Cu	0.097	0.053	0.084	0.116	0.117	0.048	0.079	0.142	2.016	0.158	0.352	6.150
Pb	0.467	0.068	0.190	0.565	0.395	0.043	0.166	0.448	2.887	0.000	1.843	7.003
Zn	0.022	0.002	0.003	0.013	0.008	0.001	0.003	0.011	0.037	0.002	0.010	0.041
Ni	2.799	2.221	2.833	3.411	2.918	2.187	2.822	3.264	3.429	1.870	3.513	4.035
Hg	1.253	1.054	1.280	1.355	1.464	1.130	1.506	1.732	1.194	0.000	1.355	2.033
HI	4.638	3.985	4.785	5.307	4.902	4.045	4.552	5.428	9.564	8.151	8.210	12.224

Q1 and Q3 represent the upper and lower quartile, respectively

Fig. 6 Box diagram of non-carcinogenic hazard quotient of different heavy metals (**a** children, **b** adult)

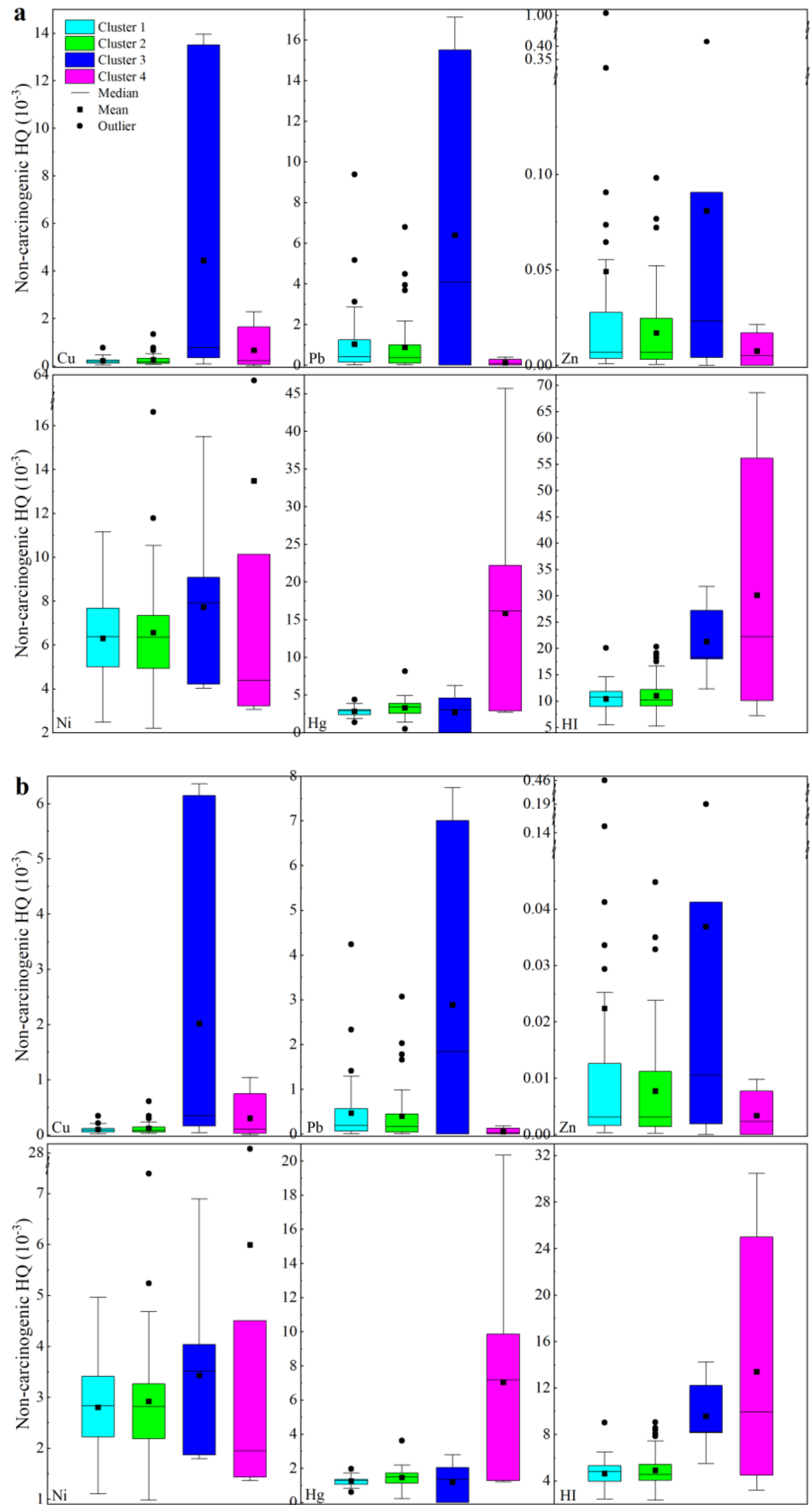
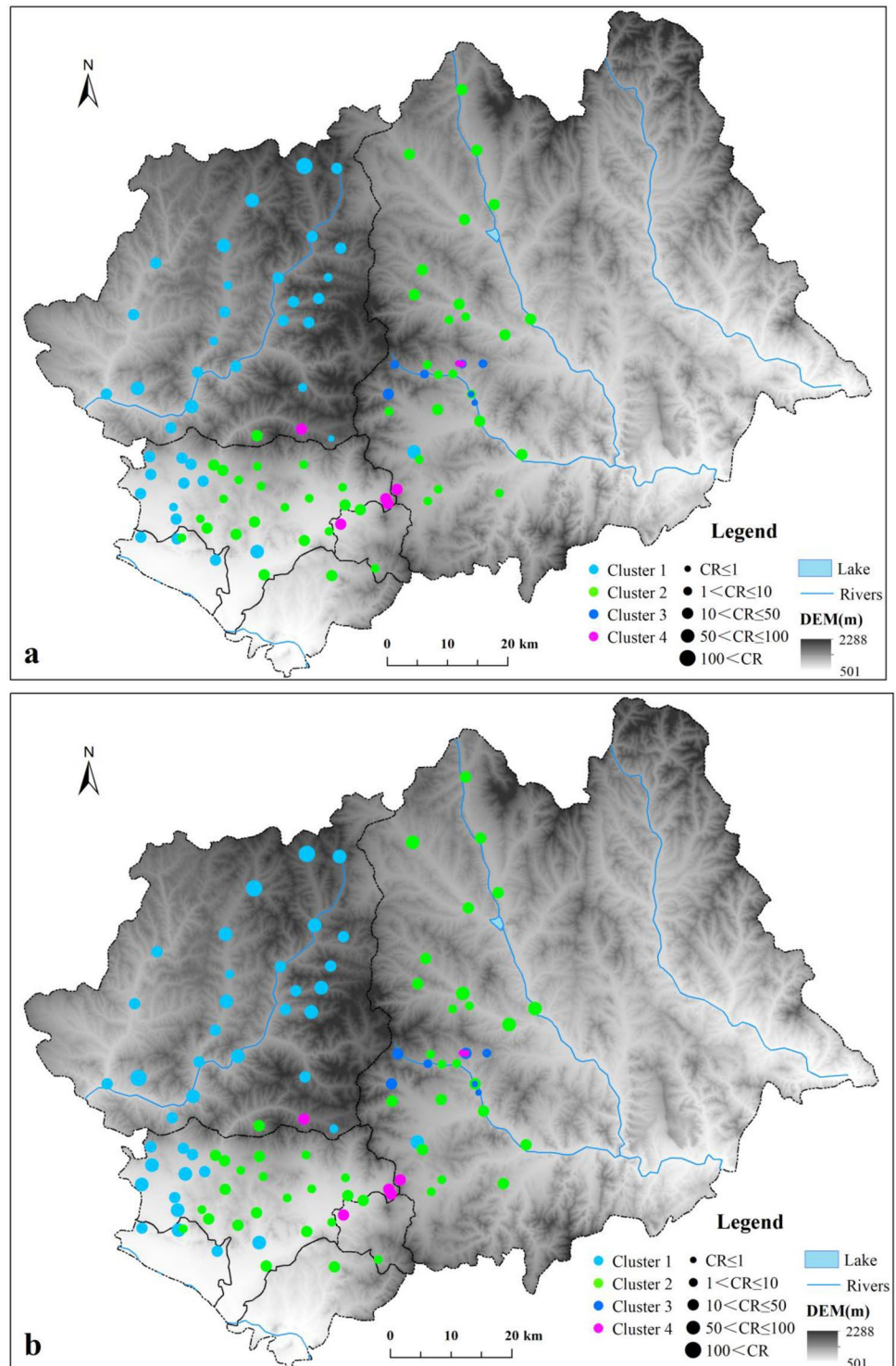


Fig. 7 Distribution characteristics of comprehensive carcinogenic health risk assessment results for different populations (**a** children, **b** adult)



non-carcinogenic hazard quotient (HQ) of heavy metals Cu, Pb, Zn, Ni, and Hg to both children and adults in each cluster showed lower risks (< 1) (Fig. 6). As such, the Non-Carcinogenic Hazard Index (HI) values to both children and adults in each cluster posed negligible health risks (Fig. 6). Interesting, contrary to carcinogenic risk results, the HI

value caused by various non-carcinogenic indicators in each cluster followed the order: Cluster 4 > Cluster 3 > Cluster 2 = Cluster 1.

Although the groundwater in Cluster 3 and 4 were located adjacent to the mine wastewater where intensive mining activities occurred, the carcinogenic health risk was not

that noticeable. Instead, groundwater in the mountain valley in the northwest and the piedmont sloping plain in the southwest of the study area where the aboveground mining activities were less frequent while buried abundant belowground mineral sources (Cluster 1), had the highest carcinogenic health risk (Fig. 7a). However, this area had the lowest non-carcinogenic health risk. Hence, the aboveground mine activities (defined as the mine wastewater contamination aboveground) mostly influenced the non-carcinogenic health risk but not much on the carcinogenic health risk. Precisely determining the sources of the heavy metals in the groundwater is extremely challenging, and past studies have found that both anthropogenic and geogenic sources affect the groundwater quality in other mine areas (Newman et al. 2017; Singh et al. 2018; Adamu et al. 2015). Additionally, we cannot rule out that the recharge and discharge of groundwater might affect this conclusion, although the groundwater flow direction (from north to south) did not show such effects.

Comprehensive Health Risk Assessment

The results of total carcinogenic risk (CR_{total}) and hazard index (HI) of heavy metals were shown in Fig. S3. Across the whole study area, the CR_{total} of Cd, As and Cr(VI) for children ranged from 5.950×10^{-6} to 2.877×10^{-5} , and the CR_{total} of 1 shallow groundwater sample exceeded the unacceptable risk level and 94% samples were greater than the acceptable risk value. For adults, the CR_{total} of the heavy metals was two times higher than that for children, and the CR_{total} of 3 samples exceeded the unacceptable risk levels and 93% of samples were greater than the acceptable risk value. Therefore, it can conclude that the overall level of carcinogenic health risks posed by Cd, As, and Cr(VI) for adults was much higher than that for children (Fig. S3).

To be noted, HI shown by these trace elements for children and adults was far below the acceptable risk level. Thus, only potential carcinogenic health risks caused by Cd, As, and Cr(VI) for children and adults should be considered when analyzing the comprehensive health risk assessment, while non-carcinogenic health risks could be removed. The high-risk samples were distributed in the river valley in the northwest of the study area, while a small number was distributed in the piedmont sloping plain in the southwest or eastern region (Fig. 7b). The population density was relatively high in these regions due to the rapid development of urbanization. Hence, it is imperative to strengthen the long-term monitoring of Cd, As, and Cr(VI) content and perform corresponding physical, chemical, and biological pretreatments (Sheng et al. 2018; Zhang et al. 2021), especially for Cr(VI) and As, to reduce the public health risk.

The authenticity of heavy metal content in groundwater samples was confirmed via the preciseness of sample

collection, storage, transportation, and the standardization of laboratory tests. However, some sources of uncertainty in the health risk assessment still exist. On one hand, it was difficult to quantify some parameters (e.g., IR, ED, BW and AT etc.) of the health risk assessment model for water environment in the actual calculation, which were all adopted from the existing empirical values or statistical average values in China's Technical Guidelines or published literature. On the other hand, the differences in demographic composition, physiology, and regional living habits were not considered, which may not conform to the actual situation of local residents in the study area. Thus, the evaluation results in the present study only represented the average health risk level of children and adults, and there may be some uncertainties in the actual risk of individual persons. However, these uncertainties did not affect the authenticity and effectiveness of the health risk assessment as previously described (He et al. 2013; Zhou et al. 2021; Su et al. 2018; Qiao et al. 2020; Fang et al. 2021). The current results were still effective and time-sensitive, which was of great scientific significance to groundwater protection, drinking water safety, and reducing health risk levels for residents in the study area and similar multi-mineral resources area.

Conclusion

The distribution of Cd, As, Cr(VI), Cu, Pb, Zn, Ni, and Hg was unraveled, and potential health risk assessment was conducted for children and adults considering different exposure pathways in the multi-mineral resources area. Groundwater in the piedmont sloping plain in the southwest of the study area had high concentrations of Cd, As, Cu, and Ni, and groundwater in the eastern mountainous and river valley had the high Cu, Pb, Zn, Ni, and Hg concentrations. Water–rock interaction was the primary underlying source of As, Pb, Ni, and Cr(VI) with some influences of mining activities, while Cd, Zn, and Hg were potentially originated from anthropogenic activities. As a result, the overall level of total carcinogenic risk for adults was much higher than that for children across the whole study area, and for both children and adults, the carcinogenic risks followed the order of $Cr(VI) > As > Cd$. Meanwhile, the non-carcinogenic risks of Cu, Pb, Zn, Ni, and Hg for both children and adults were negligible. The potential health risks for residents, especially carcinogenic risks of groundwater, were presented in the mountain valley where geogenic sources may outweigh the anthropogenic sources. Cr(VI) and As should be the primary health risk control and pretreated index in the groundwater in multi-mineral resource areas.

Supplementary Information The online version contains supplementary material available at <https://doi.org/10.1007/s12403-021-00455-z>.

Acknowledgements Not applicable.

Funding This work was financially supported by Grants from the China Geological Survey Program (DD20190820, DD20190338) and National Natural Science Foundation of China (41702262).

Data Availability Not applicable.

Declarations

Competing interests The authors declare that there is no competing interests.

References

- Adamu CI, Nganje TN, Edet A (2015) Heavy metal contamination and health risk assessment associated with abandoned barite mines in Cross River state, southeastern Nigeria. *Environ Nanotechnol Monit Manag* 3:10–21. <https://doi.org/10.1016/j.enmm.2014.11.001>
- Akcil A, Koldas S (2006) Acid Mine Drainage (AMD): causes, treatment and case studies. *J Clean Prod* 14:1139–1145. <https://doi.org/10.1016/j.jclepro.2004.09.006>
- Ameh T, Sayes CM (2019) The potential exposure and hazards of copper nanoparticles: a review. *Environ Toxicol Pharmacol* 71:103220. <https://doi.org/10.1016/j.etap.2019.103220>
- Astel A, Tsakovski S, Barbieri P, Simeonov V (2007) Comparison of self-organizing maps classification approach with cluster and principal components analysis for large environmental data sets. *Water Res* 41:4566–4578. <https://doi.org/10.1016/j.watres.2007.06.030>
- Baltasa H, Sirina M, Gökbayrak E, Özcelik AE (2020) A case study on pollution and a human health risk assessment of heavy metals in agricultural soils around Sinop province, Turkey. *Chemosphere* 241:125015. <https://doi.org/10.1016/j.chemosphere.2019.125015>
- Bempah CK, Ewusi A (2016) Heavy metals contamination and human health risk assessment around Obuasi gold mine in Ghana. *Environ Monit Assess* 188:261. <https://doi.org/10.1007/s10661-016-5241-3>
- Bodrud-Doza M, Islam S-U, Hasan MT, Alam F, Haque MM, Rakib MA, Asad MA, Rahman MA (2019) Groundwater pollution by trace metals and human health risk assessment in central west part of Bangladesh. *Groundw Sustain Dev* 9:100219. <https://doi.org/10.1016/j.gsd.2019.100219>
- Chen HY, Teng YG, Lu SJ, Wang YY, Wang JS (2015) Contamination features and health risk of soil heavy metals in China. *Sci Total Environ* 512–513:143–153. <https://doi.org/10.1016/j.scitotenv.2015.01.025>
- Chen H, Teng Y, Lu S, Wang Y, Wu J, Wang J (2016) Source apportionment and health risk assessment of trace metals in surface soils of Beijing metropolitan, China. *Chemosphere* 144:1002–1011. <https://doi.org/10.1016/j.chemosphere.2015.09.081>
- Chen IT, Chang LC, Chang FJ (2018) Exploring the spatio-temporal interrelation between groundwater and surface water by using the self-organizing maps. *J Hydrol* 556:131–142. <https://doi.org/10.1016/j.jhydrol.2017.10.015>
- Cheng PS, Weng SF, Chiang CH, Lai FJ (2016) Relationship between arsenic-containing drinking water and skin cancers in the arseniasis endemic areas in Taiwan. *J Dermatol* 43:181–186. <https://doi.org/10.1111/1346-8138.13058>
- CHNMEP (2014) Technical guidance for risk assessment of contaminated sites. (HJ 25.3-2014), Ministry of Environmental Protection of the People's Republic of China. China Environmental Science Press, Beijing (**in Chinese**)
- CHNMPH (2006) Standards for drinking water quality (GB5749-2006). Ministry of Health of the People's Republic of China, China Standards Press, Beijing (**in Chinese**)
- Choi BY, Yun ST, Kim KH, Kim JW, Kim HM, Koh YK (2014) Hydrogeochemical interpretation of South Korean groundwater monitoring data using self-organizing maps. *J Geochem Explor* 137:73–84. <https://doi.org/10.1016/j.gexplo.2013.12.001>
- Cloutier V, Lefebvre R, Therrien R, Savard MM (2008) Multivariate statistical analysis of geochemical data as indicative of the hydrogeochemical evolution of groundwater in a sedimentary rock aquifer system. *J Hydrol* 353:294–313. <https://doi.org/10.1016/j.jhydrol.2008.02.015>
- Dai LJ, Wang LQ, Li LF, Zhang Y, Ma CX, Xing BS (2018) Multivariate geostatistical analysis and source identification of heavy metals in the sediment of Poyang Lake in China. *Sci Total Environ* 2018(621):1433–1444. <https://doi.org/10.1016/j.scitotenv.2017.10.085>
- DeGraff JV (2007) Addressing the toxic legacy of abandoned mines on public land in the western United States. *Rev Eng Geol* 17:1–8. [https://doi.org/10.1130/2007.4017\(01\)](https://doi.org/10.1130/2007.4017(01))
- Dermatas D, Mpouras T, Chrysochoou M, Panagiotakis I, Vatsaris C, Linardos N, Theologou E, Boboti N, Xenidis A, Papassiopi N, Sakellariou L (2015) Origin and concentration profile of chromium in a Greek aquifer. *J Hazard Mater* 281:35–46. <https://doi.org/10.1016/j.jhazmat.2014.09.050>
- Dieter HH, Bayer TA, Multhaup G (2005) Environmental Copper and Manganese in the Pathophysiology of Neurologic Diseases (Alzheimer's Disease and Manganism). *Acta Hydrochim Hydrobiol* 33:72–78. <https://doi.org/10.1002/ahch.200400556>
- Duan XL, Zhao XG (2014) Highlights of the Chinese exposure factors handbook (Adult). China Environmental Science Press (in Chinese), Beijing
- Emenike PC, Neris JB, Tenebe IT, Nnaji CC, Jarvis P (2020) Estimation of some trace metal pollutants in River Atuwara southwestern Nigeria and spatio-temporal human health risks assessment. *Chemosphere* 239:124770. <https://doi.org/10.1016/j.chemosphere.2019.124770>
- Facchinelli A, Sacchi E, Mallen L (2001) Multivariate statistical and GIS-based approach to identify heavy metal sources in soils. *Environ Pollut* 114(3):313–324. [https://doi.org/10.1016/S0269-7491\(00\)00243-8](https://doi.org/10.1016/S0269-7491(00)00243-8)
- Fang H, Lin ZF, Fu XL (2021) Spatial variation, water quality, and health risk assessment of trace elements in groundwater in Beijing and Shijiazhuang, North China Plain. *Environ Sci Pollut Res*. <https://doi.org/10.1007/s11356-021-14557-3>
- Feng Q, Li T, Qian B, Zhou L, Gao B, Yuan T (2014) Chemical characteristics and utilization of coal mine drainage in China. *Mine Water Environ* 33(3):276–286. <https://doi.org/10.1007/s10230-014-0280-x>
- Feng F, Jia YF, Yang Y, Huan H, Lian XY, Xu XJ, Xia F, Han X, Jiang Y (2020) Hydrogeochemical and statistical analysis of high fluoride groundwater in northern China. *Environ Sci Pollut Res* 27:34840–34861. <https://doi.org/10.1007/s11356-020-09784-z>
- Fryer M, Collins CD, Ferrier H, Colville RN, Nieuwenhuijsen MJ (2006) Human exposure modelling for chemical risk assessment, a review of current approaches and research and policy implications. *Environ Sci Pol* 9:261–274. <https://doi.org/10.1016/j.envsci.2005.11.011>

- Gao B, Gao L, Gao J, Xu D, Wang Q, Sun K (2019) Simultaneous evaluations of occurrence and probabilistic human health risk associated with trace elements in typical drinking water sources from major river basins in China. *Sci Total Environ* 666:139–146. <https://doi.org/10.1016/j.scitotenv.2019.02.148>
- Giraudel J, Lek S (2001) A comparison of self-organizing map algorithm and some conventional statistical methods for ecological community ordination. *Ecol Model* 146:329–339. [https://doi.org/10.1016/S0304-3800\(01\)00324-6](https://doi.org/10.1016/S0304-3800(01)00324-6)
- Giri S, Singh AK (2014) Risk assessment, statistical source identification and seasonal fluctuation of dissolved metals in the Subarnarekha River, India. *J Hazard Mater* 265(2):305–314. <https://doi.org/10.1016/j.jhazmat.2013.09.067>
- Giri S, Singh A (2015) Human health risk assessment via drinking water pathway due to metal contamination in the groundwater of Subarnarekha River Basin. *India Environ Monit Assess* 187(3):63. <https://doi.org/10.1007/s10661-015-4265-4>
- Giri S, Singh AK (2016) Spatial distribution of metal(loid)s in groundwater of a mining dominated area: recognising metal(loid) sources and assessing carcinogenic and non-carcinogenic human health risk. *Int J Environ Anal Chem* 96(14):1313–1330. <https://doi.org/10.1080/03067319.2016.1255735>
- Goldhaber SB (2003) Trace element risk assessment: essentiality vs. toxicity. *Regul Toxicol Pharmacol* 38:232–242. [https://doi.org/10.1016/S0273-2300\(02\)00020-X](https://doi.org/10.1016/S0273-2300(02)00020-X)
- Gómez JB, Aqué LF, Gimeno MJ (2008) Sensitivity and uncertainty analysis of mixing and mass balance calculations with standard and PCA-based geochemical codes. *Appl Geochem* 23:1941–1956. <https://doi.org/10.1016/j.apgeochem.2008.02.019>
- Guney M, Zagury GJ, Dogan N, Onay TT (2010) Exposure assessment and risk characterization from trace elements following soil ingestion by children exposed to playgrounds, parks and picnic areas. *J Hazard Mater* 182(1):656–664. <https://doi.org/10.1016/j.jhazmat.2010.06.082>
- Guo H, Wen D, Liu Z, Jia Y, Guo Q (2014) A review of high arsenic groundwater in Mainland and Taiwan, China: Distribution, characteristics and geochemical processes. *Appl Geochem* 41:196–217. <https://doi.org/10.1016/j.apgeochem.2013.12.016>
- Haselbeck V, Kordilla J, Krause F, Sauter M (2019) Self-organizing maps for the identification of groundwater salinity sources based on hydrochemical data. *J Hydrol* 576:610–619. <https://doi.org/10.1016/j.jhydrol.2019.06.053>
- Hashim MA, Mukhopadhyay S, Sahu JN, Sengupta B (2011) Remediation technologies for heavy metal contaminated groundwater. *J Environ Manag* 92:2355–2388. <https://doi.org/10.1016/j.jenvman.2011.06.009>
- He B, Yun ZJ, Shi JB, Jiang GB (2013) Research progress of heavy metal pollution in China: Sources, analytical methods, status, and toxicity. *Chin Sci Bull* 58(2):134–140. <https://doi.org/10.1007/s11434-012-5541-0>
- He X, Wu J, He S (2019) Hydrochemical characteristics and quality evaluation of groundwater in terms of health risks in Luohe aquifer in Wuqi County of the Chinese Loess Plateau, northwest China. *Hum Ecol Risk Assess* 25(1–2):32–51. <https://doi.org/10.1080/10807039.2018.1531693>
- He X, Li P, Wu J, Wei M, Ren X, Wang D (2021) Poor groundwater quality and high potential health risks in the Datong Basin, northern China: Research from published data. *Environ Geochem Health* 43(2):791–812. <https://doi.org/10.1007/s10653-020-00520-7>
- Hua S, Liang J, Zeng G, Xu M, Zhang C, Yuan Y, Li X, Li P, Liu J, Huang L (2015) How to manage future groundwater resource of China under climate change and urbanization: an optimal stage investment design from modern portfolio theory. *Water Res* 85(15):31–37. <https://doi.org/10.1016/j.watres.2015.08.007>
- Huang JH, Matzner E (2006) Dynamics of organic and inorganic arsenic in the solution phase of an acidic fen in Germany. *Geochim Cosmochim Acta* 70(8):2023–2033. <https://doi.org/10.1016/j.gca.2006.01.021>
- Huang DD, Han X, Zhang F, Liu F, Shi ZM, Wang GC (2021) Reduction mechanism of hexavalent chromium in aqueous solution by sulfidated granular activated carbon. *J Clean Prod* 316:128273. <https://doi.org/10.1016/j.jclepro.2021.128273>
- IARC. International Agency for Research on Cancer (2013) Agents classified by the IARC monographs, vol. 1–109. <http://monographs.iarc.fr/ENG/Classification/index.php/>. Accessed Nov 2013
- Jampani M, Huelsmann S, Liedl R, Sonkamble S, Ahmed S, Amerasinghe P (2018) Spatiotemporal distribution and chemical characterization of groundwater quality of a wastewater irrigated system: a case study. *Sci Total Environ* 636:1089–1098. <https://doi.org/10.1016/j.scitotenv.2018.04.347>
- Jha MK, Shekhar A, Jenifer MA (2020) Assessing groundwater quality for drinking water supply using hybrid fuzzy-GIS-based water quality index. *Water Res* 179:115867. <https://doi.org/10.1016/j.watres.2020.115867>
- Jia Z, Li S, Wang L (2018) Assessment of soil heavy metals for environment and human health in a rapidly urbanization area of the upper Yangtze Basin. *Sci Rep* 8:3256. <https://doi.org/10.1038/s41598-018-21569-6>
- Jiang Y, Chao S, Liu J, Yue Y, Chen Y, Zhang A, Cao H (2017) Source apportionment and health risk assessment of heavy metals in soil for a township in Jiangsu Province, China. *Chemosphere* 168:1658–1668. <https://doi.org/10.1016/j.chemosphere.2016.11.088>
- Jiang W, Wang G, Sheng Y, Shi Z, Zhang H (2019) Isotopes in groundwater (^2H , ^{18}O , ^{14}C) revealed the climate and groundwater recharge in the Northern China. *Sci Total Environ* 666:298–307. <https://doi.org/10.1016/j.scitotenv.2019.02.245>
- Jiang CL, Zhao Q, Zheng LG, Chen X, Li C, Ren MX (2021a) Distribution, source and health risk assessment based on the Monte Carlo method of heavy metals in shallow groundwater in an area affected by mining activities, China. *Ecotol Environ Safe* 224:112679. <https://doi.org/10.1016/j.ecoenv.2021.112679>
- Jiang W, Sheng Y, Liu H, Ma Z, Song Y, Liu F, Chen S, Bai Y (2021b) Groundwater quality assessment and hydrogeochemical processes in typical watersheds in Zhangjiakou city, northern China. *Environ Sci Pollut Res*. <https://doi.org/10.1007/s11356-021-15644-1>
- Kefeni KK, Msagati TAM, Mamba BB (2017) Acid mine drainage: prevention, treatment options, and resource recovery: a review. *J Clean Prod* 151:475–493. <https://doi.org/10.1016/j.jclepro.2017.03.082>
- Khawal R, Mor S (2019) Distribution and health risk assessment of arsenic and selected heavy metals in Groundwater of Chandigarh, India. *Environ Pollut* 250:820–830. <https://doi.org/10.1016/j.envpol.2019.03.080>
- Khaska M, Corinne LGLS, Sassine L, Cary L, Bruguier O, Verdoux P (2018) Arsenic and metallic trace elements cycling in the surface water-groundwater-soil continuum down-gradient from a reclaimed mine area: isotopic imprints. *J Hydrol* 558:341–355. <https://doi.org/10.1016/j.jhydrol.2018.01.031>
- Khodapanah L, Sulaiman WNA, Khodapanah N (2009) Groundwater quality assessment for different purposes in Eshtehard District, Tehran, Iran. *Eur J Sci Res* 36(4):543–553
- Kim E, Little JC, Chiu N (2004) Estimating exposure to chemical contaminants in drinking water. *Environ Sci Technol* 38:1799–1806. <https://doi.org/10.1021/es026300t>
- Kim KH, Yun ST, Yu S, Choi BY, Kim MJ, Lee KJ (2020) Geochemical pattern recognitions of deep thermal groundwater in South Korea using self-organizing map: Identified pathways of

- geochemical reaction and mixing. *J Hydrol* 589:15202. <https://doi.org/10.1016/j.jhydrol.2020.125202>
- Kohonen T (1982) Self-organized formation of topologically correct feature maps. *Biol Cybern* 43:59–69
- Larson LN, Fitzgerald M, Singha K, Gooseff MN, Macalady JL, Burgos W (2013) Hydrogeochemical niches associated with hyporheic exchange beneath an acid mine drainage-contaminated stream. *J Hydrol* 501:163–174. <https://doi.org/10.1016/j.jhydrol.2013.08.007>
- Lee CSL, Li XD, Zhang G, Li J, Ding AJ, Wang T (2007) Heavy metals and Pb isotopic composition of aerosols in urban and suburban areas of Hong Kong and Guangzhou, South China—Evidence of the long-range transport of air contaminants. *Atmos Environ* 41:432–447. <https://doi.org/10.1016/j.atmosenv.2006.07.035>
- Lee J, Pedersen AB, Thomsen M (2013) Framework for combining reach and national regulations to obtain equal protection levels of human health and the environment in different countries—comparative study of Denmark and Korea. *J Environ Manag* 125:105–116. <https://doi.org/10.1016/j.jenvman.2013.07.015>
- Lee KJ, Yun ST, Yu S, Kim KH, Lee JH, Lee SH (2019) The combined use of self-organizing map technique and fuzzy c-means clustering to evaluate urban groundwater quality in Seoul metropolitan city, South Korea. *J Hydrol* 569:685–697. <https://doi.org/10.1016/j.jhydrol.2018.12.031>
- Li YL, Liu JL, Cao ZG, Lin C, Yang ZF (2010) Spatial distribution and health risk of heavy metals and polycyclic aromatic hydrocarbons (PAHs) in the water of the Luanhe River Basin, China. *Environ Monit Assess* 163(1–4):1–13. <https://doi.org/10.1007/s10661-009-0811-2>
- Li ZY, Ma ZW, Van der Kuijp TJ, Yuan ZW, Huang L (2014) A review of soil heavy metal pollution from mines in China, pollution and health risk assessment. *Sci Total Environ* 468:843–853. <https://doi.org/10.1016/j.scitotenv.2013.08.090>
- Li P, Li X, Meng X, Li M, Zhang Y (2016) Appraising groundwater quality and health risks from contamination in a semiarid region of northwest China. *Expo Health* 8(3):361–379. <https://doi.org/10.1007/s12403-016-0205-y>
- Li P, Tian R, Xue C, Wu J (2017) Progress, opportunities, and key fields for groundwater quality research under the impacts of human activities in China with a special focus on western China. *Environ Sci Pollut Res* 24(15):13224–13234. <https://doi.org/10.1007/s11356-017-8753-7>
- Li PY, He X, Li Y, Xiang G (2019) Occurrence and health implication of fluoride in groundwater of loess aquifer in the Chinese Loess Plateau: a case study of Tongchuan, Northwest China. *Expo Health* 11(2):95–107. <https://doi.org/10.1007/s12403-018-0278-x>
- Li J, Shi ZM, Wang GC, Liu F (2020) Evaluating spatiotemporal variations of groundwater quality in Northeast Beijing by Self-organizing Map. *Water* 12(5):1382. <https://doi.org/10.3390/w12051382>
- Li J, Wang GC, Liu F, Cui LF, Jiao YJ (2021) Supplementary material source apportionment and ecological-health risks assessment of heavy metals in topsoils near a factory, central China. *Expo Health* 13:79–92. <https://doi.org/10.1007/s12403-020-00363-8>
- Liao F, Wang GC, Shi ZM, Huang XJ, Xu FF, Xu QY, Guo L (2018) Distributions, sources, and species of heavy metals/trace elements in shallow groundwater around the Poyang Lake, East China. *Expo Health* 10:211–227. <https://doi.org/10.1007/s12403-017-0256-8>
- Lidman F, Mörth CM, Björkvald L, Laudon H (2011) Selenium dynamics in boreal streams, the role of wetlands and changing groundwater tables. *Environ Sci Technol* 45(7):2677–2683. <https://doi.org/10.1021/es102885z>
- Linou A, Petralias A, Christophi CA, Christoforidou E, Kouroutou P, Stolidis M, Veloudaki A, Tzala E, Makris KC, Karagas MR (2011) Oral ingestion of hexavalent chromium through drinking water and cancer mortality in an industrial area of Greece—an ecological study. *Environ Health* 10:50. <https://doi.org/10.1186/1476-069X-10-50>
- Liu N, Ni T, Xia J, Dai M, He C, Lu G (2010) Noncarcinogenic risks induced by metals in drinking source water of Jiangsu Province, China. *Environ Monit Assess* 177(1–4):449–456. <https://doi.org/10.1007/s10661-010-1646-6>
- Liu X, Shi H, Bai Z, Zhou W, Liu K, Wang M, He Y (2020a) Heavy metal concentrations of soils near the large opencast coal mine pits in China. *Chemosphere* 244:125360. <https://doi.org/10.1016/j.chemosphere.2019.125360>
- Liu Y, Sheng Y, Feng C, Chen N, Liu T (2020b) Distinct functional microbial communities mediating the heterotrophic denitrification in response to the excessive Fe(II) stress in groundwater under wheat-rice stone and rock phosphate amendments. *Environ Res* 185:109391. <https://doi.org/10.1016/j.envres.2020.109391>
- Lorite-Herrera M, Jiménez-Espinosa R, Jiménez-Millán J, Hiscock KM (2008) Integrated hydrochemical assessment of the Quaternary alluvial aquifer of the Guadalquivir River, southern Spain. *Appl Geochem* 23:2040–2054. <https://doi.org/10.1016/j.apgeochem.2008.03.013>
- Lv JS, Liu Y, Zhang ZL, Dai J, Dai B, Zhu Y (2015) Identifying the origins and spatial distributions of heavy metals in soils of Ju county (Eastern China) using multivariate and geostatistical approach. *J Soils Sediments* 15(1):163–178. <https://doi.org/10.1007/s11368-014-0937-x>
- Mazhar I, Hamid A, Afzal S (2019) Groundwater quality assessment and human health risks in Gujranwala District, Pakistan. *Environ Earth Sci* 78(22):1–12. <https://doi.org/10.1007/s12665-019-8644-y>
- Miguel ED, Iribarren I, Chacón E, Ordoñez A, Charlesworth S (2007) Risk-based evaluation of the exposure of children to trace elements in playgrounds in Madrid (Spain). *Chemosphere* 66(3):505–513. <https://doi.org/10.1016/j.chemosphere.2006.05.065>
- Mohan D, Pittman CU Jr (2006) Activated carbons and low cost adsorbents for remediation of tri- and hexavalent chromium from water. *J Hazard Mater* 137(2):762–811. <https://doi.org/10.1016/j.jhazmat.2006.06.060>
- Moore PJ, Martin JB, Sreaton EJ (2009) Geochemical and statistical evidence of recharge, mixing, and controls on spring discharge in an eogenetic karst aquifer. *J Hydrol* 376:443–455. <https://doi.org/10.1016/j.jhydrol.2009.07.052>
- Morales KH, Ryan L, Kuo TL, Wu MM, Chen CJ (2000) Risk of internal cancers from arsenic in drinking water. *Environ Health Persp* 108(7):655–661. <https://doi.org/10.1289/ehp.00108655>
- Muhammad S, Shah MT, Khan S (2011) Health risk assessment of heavy metals and their source apportionment in drinking water of Kohistan region, northern Pakistan. *Microchem J* 98:334–343. <https://doi.org/10.1016/j.microc.2011.03.003>
- Mukherjee I, Singh UK, Singh RP, Anshumali, Kumari AD, Jha PK, Mehta P (2020) Characterization of heavy metal pollution in an anthropogenically and geologically influenced semi-arid region of east India and assessment of ecological and human health risks. *Sci Total Environ* 705:135801. <https://doi.org/10.1016/j.scitotenv.2019.135801>
- Nath BK, Chaliha C, Bhuyan B, Kalita E, Baruah DC, Bhagabati AK (2018) Gis mapping-based impact assessment of groundwater contamination by arsenic and other heavy metal contaminants in the Brahmaputra River valley: a water quality assessment study. *J Clean Prod* 201:1001–1011. <https://doi.org/10.1016/j.jclepro.2018.08.084>
- Newman C, Agioutantis Z, Boede G, Leon J (2017) Assessment of potential impacts to surface and subsurface water bodies due to

- longwall mining. *Int J Min Sci Technol* 27:57–64. <https://doi.org/10.1016/j.ijmst.2016.11.016>
- Pan L, Wang Y, Ma J, Hu Y, Su B, Fang G, Wang L, Xiang B (2018) A review of heavy metal pollution levels and health risk assessment of urban soils in Chinese cities. *Environ Sci Pollut Res* 25:1055–1069. <https://doi.org/10.1007/s11356-017-0513-1>
- Pareja-Carrera J, Mateo R, Rodríguez-Estival J (2014) Lead (Pb) in sheep exposed to mining pollution: implications for animal and human health. *Ecotoxicol Environ Saf* 108:210–216. <https://doi.org/10.1016/j.ecoenv.2014.07.014>
- Park RM, Bena JF, Stayner LT, Smith RJ, Gibb HJ, Lees PS (2004) Hexavalent chromium and lung cancer in the chromate industry: a quantitative risk assessment. *Risk Anal* 24(5):1099–1108. <https://doi.org/10.1111/j.0272-4332.2004.00512.x>
- Park YS, Kwon YS, Hwang SJ, Park S (2014) Characterizing effects of landscape and morphometric factors on water quality of reservoirs using a self-organizing map. *Environ Model Softw* 55:214–221. <https://doi.org/10.1016/j.envsoft.2014.01.031>
- Podgorski JE, Eqani S, Khanam T, Ullah R, Shen H, Berg M (2017) Extensive arsenic contamination in high-pH unconfined aquifers in the Indus Valley. *Sci Adv* 3(8):e1700935. <https://doi.org/10.1126/sciadv.1700935>
- Qiao JB, Zhua YJ, Jia XX, Shao MA, Niu XQ, Liu JY (2020) Distributions of arsenic and other heavy metals, and health risk assessments for groundwater in the Guanzhong Plain region of China. *Environ Res* 181:108957. <https://doi.org/10.1016/j.envres.2019.108957>
- Qu S, Wang G, Shi Z, Xu Q, Guo Y, Ma L, Sheng Y (2018) Using stable isotopes (δD , $\delta^{18}O$, $\delta^{34}S$ and $^{87}Sr/^{86}Sr$) to identify sources of water in abandoned mines in the Fengfeng coal mining district, northern China. *Hydrogeol J* 26(5):1443–1453. <https://doi.org/10.1007/s10040-018-1803-5>
- Qu S, Shi ZM, Liang XY, Wang GC, Han JQ (2021) Multiple factors control groundwater chemistry and quality of multi-layer groundwater system in Northwest China coalfield-Using self-organizing maps (SOM). *J Geochem Explor* 227:106795. <https://doi.org/10.1016/j.gexplo.2021.106795>
- Rakhunde R, Deshpande L, Juneja HD (2012) Chemical speciation of chromium in water: a review. *Crit Rev Environ Sci Technol* 42:776–810
- Ravindra K, Garg VK (2007) Hydro-chemical survey of groundwater of hisar city and assessment of defluoridation methods used in India. *Environ Monit Assess* 132:33–43. <https://doi.org/10.1007/s10661-006-9500-6>
- Ravindra K, Mor S (2019) Distribution and health risk assessment of arsenic and selected heavy metals in Groundwater of Chandigarh, India. *Environ Pollut* 250:820–830. <https://doi.org/10.1016/j.envpol.2019.03.080>
- Ravindra K, Thind PS, Mor S, Singh T, Mor S (2019) Evaluation of groundwater contamination in Chandigarh: source identification and health risk assessment. *Environ Pollut* 255(Pt 1):113062. <https://doi.org/10.1016/j.envpol.2019.113062>
- Riederer AM, Belova A, George BJ, Anastas PT (2013) Urinary cadmium in the 1999–2008 U.S. National Health and Nutrition Examination Survey (NHANES). *Environ Sci Technol* 47:1137–1147. <https://doi.org/10.1021/es303556n>
- Robles-Camacho J, Armienta MA (2000) Natural chromium contamination of groundwater at León Valley, México. *J Geochem Explor* 68:167–181. [https://doi.org/10.1016/S0375-6742\(99\)00083-7](https://doi.org/10.1016/S0375-6742(99)00083-7)
- Šajin R, Halamić J, Peh Z, Galović L, Alijagić J (2011) Assessment of the natural and anthropogenic sources of chemical elements in alluvial soils from the Drava River using multivariate statistical methods. *J Geochem Explor* 110(3):278–289. <https://doi.org/10.1016/j.gexplo.2011.06.009>
- Sako A, Bamba O, Gordio A (2016) Hydrogeochemical processes controlling groundwater quality around Bomboré gold mineralized zone, Central Burkina Faso. *J Geochem Explor* 170:58–71. <https://doi.org/10.1016/j.gexplo.2016.08.009>
- Sheng Y, Bibby K, Grettenberger C, Kaley B, Macalady JL, Wang G, Burgos WD (2016) Geochemical and temporal influences on the enrichment of acidophilic iron-oxidizing bacterial communities. *Appl Environ Microbiol* 82(12):3611–3621. <https://doi.org/10.1128/AEM.00917-16>
- Sheng Y, Kaley B, Bibby K, Grettenberger C, Macalady JL, Wang G, Burgos WD (2017) Bioreactors for low-pH iron(II) oxidation remove considerable amounts of total iron. *RSC Adv* 7:35962–35972. <https://doi.org/10.1039/C7RA03717A>
- Sheng Y, Zhang X, Zhai X, Zhang F, Li G, Zhang D (2018) A mobile modular and rapidly-acting treatment system for optimizing and improving the removal of non-aqueous phase liquids (NAPLs) in groundwater. *J Hazard Mater* 360:639–650. <https://doi.org/10.1016/j.jhazmat.2018.08.044>
- Sheng Y, Liu Y, Ma L, Deng S, Yang M, Liu Y, Li G, Zhang D (2021) Distinct assembly processes shape bacterial communities along unsaturated, groundwater fluctuated, and saturated zones. *Sci Total Environ* 761:143303. <https://doi.org/10.1016/j.scitotenv.2020.143303>
- Shil S, Singh UK (2019) Health risk assessment and spatial variations of dissolved heavy metals and metalloids in a tropical river basin system. *Ecol Indic* 106:105455. <https://doi.org/10.1016/j.ecoli.2019.105455>
- Siddiqui AU, Jain MK, Mastro RE (2020) Pollution evaluation, spatial distribution, and source apportionment of trace metals around coal mines soil: the case study of eastern India. *Environ Sci Pollut Res Int* 27:10822–10834. <https://doi.org/10.1007/s11356-019-06915-z>
- Singh UK, Kumar B (2017) Pathways of heavy metals contamination and associated human health risk in Ajay River basin, India. *Chemosphere* 174:183–199. <https://doi.org/10.1016/j.chemosphere.2017.01.103>
- Singh UK, Ramanathan AL, Subramanian V (2018) Groundwater chemistry and human health risk assessment in the mining region of East Singhbhum, Jharkhand, India. *Chemosphere* 204:501–513. <https://doi.org/10.1016/j.chemosphere.2018.04.060>
- Song QB, Li JH (2015) A review on human health consequences of metals exposure to e-waste in China. *Environ Pollut* 196:450–461. <https://doi.org/10.1016/j.envpol.2014.11.004>
- Su H, Kang W, Xu Y, Wang J (2018) Assessing groundwater quality and health risks of nitrogen pollution in the Shenfu Mining Area of Shaanxi Province, Northwest China. *Expo Health* 10:77–97. <https://doi.org/10.1007/s12403-017-0247-9>
- Su H, Wang J, Liu J (2019) Geochemical factors controlling the occurrence of high-fluoride groundwater in the western region of the Ordos basin, northwestern China. *Environ Pollut* 252(Pt B):1154–1162. <https://doi.org/10.1016/j.envpol.2019.06.046>
- Sun J, Tang C, Wu P, Strosnider WH (2014) Hydrogen and oxygen isotopic composition of karst waters with and without acid mine drainage: impacts at a Sw China coalfield. *Sci Total Environ* 487:123–129. <https://doi.org/10.1016/j.scitotenv.2014.04.008>
- Sun S, Xie X, Li J, Qian K, Chi Z (2020) Distribution and formation of thioarsenate in high arsenic groundwater from the Datong Basin, northern China. *J Hydrol* 590:125268. <https://doi.org/10.1016/j.jhydrol.2020.125268>
- Tong SM, Li HR, Tudi M, Yuan X, Yang LS (2021) Comparison of characteristics, water quality and health risk assessment of trace elements in surface water and groundwater in China. *Ecotox Environ Safe* 219:112283. <https://doi.org/10.1016/j.ecoenv.2021.112283>
- Tseng CH, Lei C, Chen YC (2018) Evaluating the health costs of oral hexavalent chromium exposure from water pollution: a case study

- in Taiwan. *J Clean Prod* 172:819–826. <https://doi.org/10.1016/j.jclepro.2017.10.177>
- USEPA (2004) Risk Assessment Guidance for Superfund Volume I, Human Health Evaluation Manual (Part E, Supplemental Guidance for Dermal Risk Assessment) Final. Office of Superfund Remediation and Technology Innovation U.S. Environmental Protection Agency, Washington DC, USA
- USEPA (2011) Exposure Factors Handbook, final ed. US Environmental Protection Agency, Washington, DC [EPA/600/R-09/052F]
- USEPA (2013) Region IX, regional screening levels (formerly PRGs). San Francisco, CA 94105. www.epa.gov/region9/superfund/prg/
- USEPA (2017) Risk Assessment Guidance for Superfund (RAGS), Part A [EB/OL]. (2017-01-19) [2017-06-24]. www.epa.gov/risk/risk-assessment-guidance-superfund-rags-part
- Vesanto J, Himberg J, Alhoniemi E, Parhankagas J (2000) SOM Toolbox for Matlab 5. Report A57. <http://www.cis.hut.fi/projects/somtoolbox/>
- Wang Y, Jiao JJ, Zhang K, Zhou YZ (2016) Enrichment and mechanisms of heavy metal mobility in a coastal quaternary groundwater system of the Pearl River Delta, China. *Sci Total Environ* 545–546:493–502. <https://doi.org/10.1016/j.scitotenv.2015.12.019>
- Wang C, Lek S, Lai Z, Tudesque L (2017a) Morphology of Aulacoseira filaments as indicator of the aquatic environment in a large subtropical river: the Pearl River, China. *Ecol Indic* 81:325–332. <https://doi.org/10.1016/j.ecolind.2017.06.020>
- Wang J, Liu GJ, Liu HQ, Lam PKS (2017b) Multivariate statistical evaluation of dissolved trace elements and a water quality assessment in the middle reaches of Huaihe River, Anhui, China. *Sci Total Environ* 583:421–431. <https://doi.org/10.1016/j.scitotenv.2017.01.088>
- Wang Z, Guo H, Xiu W, Wang J, Shen M (2018) High arsenic groundwater in the Guide basin, northwestern China, Distribution and genesis mechanisms. *Sci Total Environ* 640–641:194–206. <https://doi.org/10.1016/j.scitotenv.2018.05.255>
- Wang J, Su J, Li Z, Liu B, Cheng G, Jiang Y, Li Y, Zhou S, Yuan W (2019a) Source apportionment of heavy metal and their health risks in soil-dustfall-plant system nearby a typical non-ferrous metal mining area of Tongling, Eastern China. *Environ Pollut* 254:113089. <https://doi.org/10.1016/j.envpol.2019.113089>
- Wang S, Cai L, Wen H, Luo J, Wang Q, Liu X (2019b) Spatial distribution and source apportionment of heavy metals in soil from a typical county-level city of Guangdong Province, China. *Sci Total Environ* 655:92–101. <https://doi.org/10.1016/j.scitotenv.2018.11.244>
- Wang Z, Guo H, Xing SP, Liu HY (2021) Hydrogeochemical and geothermal controls on the formation of high fluoride groundwater. *J Hydrol* 598:126372. <https://doi.org/10.1016/j.jhydrol.2021.126372>
- WHO (2011) Guidelines for drinking water quality, 4th edn. World Health Organization, Geneva
- Wu J, Sun Z (2016) Evaluation of shallow groundwater contamination and associated human health risk in an alluvial plain impacted by agricultural and industrial activities, Mid-west China. *Expo Health* 8(3):311–329. <https://doi.org/10.1007/s12403-015-0170-x>
- Wu C, Wu X, Qian C, Zhu G (2018) Hydrogeochemistry and groundwater quality assessment of high fluoride levels in the Yanchi endorheic region, northwest China. *Appl Geochem* 98:404–417. <https://doi.org/10.1016/j.apgeochem.2018.10.016>
- Wu J, Zhou H, He S, Zhang Y (2019) Comprehensive understanding of groundwater quality for domestic and agricultural purposes in terms of health risks in a coal mine area of the Ordos basin, north of the Chinese Loess Plateau. *Environ Earth Sci* 78(15):446. <https://doi.org/10.1007/s12665-019-8471-1>
- Xiao J, Wang L, Deng L, Jin Z (2019) Characteristics, sources, water quality and health risk assessment of trace elements in river water and well water in the Chinese Loess Plateau. *Sci Total Environ* 650(Pt 2):2004–2012. <https://doi.org/10.1016/j.scitotenv.2018.09.322>
- Yang X, Duan J, Wang L, Li W, Guan J, Beecham S, Mulcahy D (2015) Heavy metal pollution and health risk assessment in the Wei River in China. *Environ Monit Assess* 187(3):1–11. <https://doi.org/10.1007/s10661-014-4202-y>
- Yuan TH, Lian B, Tsai KY, Chang TK, Chiang CT, Su CC, Hwang YH (2011) Possible association between nickel and chromium-oral cancer: a case-control study in central Taiwan. *Sci Total Environ* 409:1046–1052. <https://doi.org/10.1016/j.scitotenv.2010.11.038>
- Zeng X, Liu Y, You S, Zeng G, Tan X, Hu X, Li F (2015) Spatial distribution, health risk assessment and statistical source identification of the trace elements in surface water from the Xiangjiang River, China. *Environ Sci Pollut Res Int* 22(12):9400–9412. <https://doi.org/10.1007/s11356-014-4064-4>
- Zeng B, Zhang Z, Yang M (2018) Risk assessment of groundwater with multisource pollution by a long-term monitoring programme for a large mining area. *Int Biodeterior Biodegrad* 128:100–108. <https://doi.org/10.1016/j.ibiod.2017.01.002>
- Zhang Y, Wang XX (2021) Evaluation of heavy metal pollution in shallow groundwater of farmland in Huaibei Plain. *China ICESCE* 267:02009. <https://doi.org/10.1051/e3sconf/202126702009>
- Zhang SZ, Liu GJ, Sun RY, Wu D (2016) Health risk assessment of heavy metals in groundwater of coal mining area: a case study in Dingji coal mine, Huainan coalfield. *China Hum Ecol Risk Assess* 22(7):1469–1479. <https://doi.org/10.1080/10807039.2016.1185689>
- Zhang Y, Wu J, Xu B (2018) Human health risk assessment of groundwater nitrogen pollution in Jinghui canal irrigation area of the loess region, northwest China. *Environ Earth Sci* 77(7):273. <https://doi.org/10.1007/s12665-018-7456-9>
- Zhang B, Liu J, Sheng Y, Shi J, Dong H (2021) Disentangling microbial syntrophic mechanisms for hexavalent chromium reduction in autotrophic biosystems. *Environ Sci Technol* 55(9):6340–6351. <https://doi.org/10.1021/acs.est.1c00383>
- Zhao ZQ, Zhu YG, Li HY, Smith SE, Smith FA (2004) Effects of forms and rates of potassium fertilizers on cadmium uptake by two cultivars of spring wheat (*Triticum aestivum* L.). *Environ Int* 29(7):973–978. [https://doi.org/10.1016/S0160-4120\(03\)00081-3](https://doi.org/10.1016/S0160-4120(03)00081-3)
- Zhou L, Liu G, Shen M, Hu R, Sun M, Liu Y (2019) Characteristics and health risk assessment of heavy metals in indoor dust from different functional areas in Hefei, China. *Environ Pollut* 251:841–849. <https://doi.org/10.1016/j.envpol.2019.05.058>
- Zhou Y, Li P, Chen M, Dong Z, Lu C (2021) Groundwater quality for potable and irrigation uses and associated health risk in southern part of Gu'an County, North China. *Plain Environ Geochem Health* 43(2):813–835. <https://doi.org/10.1007/s10653-020-00553-y>
- Zhu G, Wu X, Ge J, Liu F, Zhao W, Wu C (2020) Influence of mining activities on groundwater hydrochemistry and heavy metal migration using a self-organizing map (SOM). *J Cleaner Prod* 257:120664. <https://doi.org/10.1016/j.jclepro.2020.120664>

Publisher's Note Springer Nature remains neutral with regard to jurisdictional claims in published maps and institutional affiliations.